applied sciences

MDPI

Article

Development of a System for Cyclic Shear Tests on Full-Scale Walls

Leandro Di Gregorio [1,2,*], Aníbal Costa [2], Hugo Rodrigues [2], Jorge Fonseca [2] and Alice Tavares Costa [3]

[1] Environmental Engineering Graduate Program, Urban Engineering Graduate Program, Civil Construction Department, Polytechnic School, Federal University of Rio de Janeiro, Rio de Janeiro 21941-901, Brazil
[2] RISCO—Aveiro Research Centre for Risks and Sustainability in Construction, Civil Engineering Department, University of Aveiro, 3810-193 Aveiro, Portugal; agc@ua.pt (A.C.); hrodrigues@ua.pt (H.R.); jfonseca@ua.pt (J.F.)
[3] Department of Materials and Ceramic Engineering, CICECO—Aveiro Institute of Materials, University of Aveiro, 3810-193 Aveiro, Portugal; tavares.c.alice@ua.pt
* Correspondence: leandro.torres@poli.ufrj.br

Featured Application: Providing cyclic shear tests for full-scale walls.

Abstract: The SHS-Multirisk Project proposes a residence model that is simultaneously resistant to earthquakes and hurricanes within a specific range of magnitude to be defined in the project. It uses simple, low-cost, and environmentally friendly construction technologies compared with traditional alternatives or more technological, but less accessible ones. To reach the SHS-Multirisk objectives, an experimental campaign to carry on cyclic shear tests involved a set of 15 reinforced soil-cement compressed earth block walls. Within this program, a particular test system was developed, conditioned by the guidelines: simplicity, availability of resources (especially components, equipment, and workmanship), rationalization of the available space, and scalability of the tests. Considering the short time available for designing and manufacturing the test system and for carrying out the shear tests, it was decided to adopt a project management framework in Scrum mode. This article presents the system developed to conduct full-scale cyclic shear (combined with bending) tests on walls, exploring its characteristics, the development process, the experiment execution process, and a basic analysis of the main test outputs.

Keywords: seismic; cyclic shear tests; shear combined with bending; development of a test system; test setup; disaster risk reduction

Citation: Di Gregorio, L.; Costa, A.; Rodrigues, H.; Fonseca, J.; Tavares Costa, A. Development of a System for Cyclic Shear Tests on Full-Scale Walls. *Appl. Sci.* **2023**, *13*, 7498. https://doi.org/10.3390/app13137498

Academic Editor: Raffaele Zinno

Received: 30 May 2023
Revised: 18 June 2023
Accepted: 22 June 2023
Published: 25 June 2023

1. Introduction

Losses and damages from geological threats have grown rapidly, reaching around 15,000 victims per year, which is not due to the increase in seismic activity, but rather to the increase in vulnerable settlements [1]. Simultaneously, climate change is a global reality [2] and requires adaptations of the built environment to adverse climatic scenarios, such as the incidence of hurricanes and tornadoes.

According to the World Risk Report 2018 [3], which analyzes the probability of the occurrence of earthquakes, tsunamis, hurricanes, and floods in 172 countries and their capacity to respond to events such as this, the 15 countries that present the highest risk, (on a scale of 100) are Vanuatu, Tonga, Philippines, Solomon Islands, Guyana, Papua New Guinea, Guatemala, Brunei, Bangladesh, Fiji, Costa Rica, Cambodia, East Timor, El Salvador, and Kiribati. In addition, Mexico, Chile, Sri Lanka, Indonesia, India, Pakistan, Thailand, and China, among other countries, also deserve mention regarding seismic hazards and vulnerable populations. Furthermore, in developing countries, many people live in non-engineered low-rise constructions made of poor materials, which makes them more vulnerable [4].

The SHS (Simple Housing Solution) project consists of a methodology for (re)building homes and other small buildings, in a joint working system (community construction), seeking to optimize available resources and contribute to the organization in critical situations of installed chaos, such as post-disaster, post-conflict, refugee relocation, or even in risk mitigation [5]. It is based on the fundamental principles for the sustainable restoration of housing declared by the United Nations Development Program (UNDP) and the International Platform for Recovery (IRP): environmental, technical, financial, and socio-organizational sustainability. The project was one of the 16 finalists for the 2019 Sasakawa Awards and is aligned with the Sendai Framework for Disaster Risk Reduction [6], impacting several sustainable development goals.

SHS-Multirisk is a spin-off project under development through a partnership between the Federal University of Rio de Janeiro (UFRJ) and the University of Aveiro (UA). It proposes a residence model that is simultaneously resistant to earthquakes and hurricanes within a specific magnitude range to be defined in the project. It uses simple, low-cost, and environmentally friendly construction technologies compared with traditional alternatives or more technological, but less accessible ones. In its current phase, the first SHS-Multirisk house model [7] is being improved, aiming at more aggressive scenarios.

The outcomes from SHS-Multirisk will be used to inform policies on mitigation strategies towards effective decision making for housing in critical events, with minimal resources. By doing so, SHS-Multirisk responds to the United Nations' call [8] to raise stakeholders' awareness and invest in the possible accumulated local knowledge, strengthening core competencies to contribute to urban resilience. This can be combined with the disaster mitigation and recovery processes, which should be prepared and skilled before the harmful event, as proposed by the United Nations Educational, Scientific, and Cultural Organization (UNESCO) for recognized places, following the statements confirmed by the 2009 Global Assessment Report on Disaster Risk Reduction, Risk, and Poverty in a Changing Climate [9]. The number of disasters around the world increases every year. To a great extent, this is due to growing exposure in terms of people and assets caused by rapid economic development and urban growth in cyclone coastal areas and earthquake-prone cities [10], confirming the need to implement this SHS-Multirisk project.

The potential of compressed earth blocks (CEBs) reinforced masonry technology to be applied in humanitarian emergencies and multi-hazard resilient construction is high, mainly due to the environmental, economic, and social advantages resulting from the use of local materials with a low environmental impact and the use of the beneficiaries' labor in the construction works [11]. However, there are limits to this technology that need to be better known to build resiliently as, for example, the in-plane and out-of-plane shear behavior, considering they represent a limiting factor for masonry under seismic loads [12]. Nevertheless, the NIKER (New Integrated Knowledge Based Approaches to the Protection of Cultural Heritage from Earthquake-Induced Risk) project [13] focuses its experimental analyses on earthen structures and their strengthening to face earthquake events, validating other ways for their preservation in risk areas.

To reach the SHS-Multirisk objectives, an experimental campaign to carry out on cyclic shear tests was performed at the Civil Engineering Department of UA (DECIVIL), involving 15 reinforced soil–cement compressed earth block walls. Within this program, a particular test system for full-scale specimens was developed, conditioned by the guidelines: simplicity, availability of resources (especially components, equipment, and workmanship), rationalization of the available space, and scalability of the tests in the available time.

This article aims to present the system developed to conduct full-scale cyclic shear (combined with bending) tests on walls (or other structural elements), discussing its characteristics, the development process, the experiment execution process, and providing a fundamental analysis of the main test outputs.

Shear Test Types of Setup and Their Characteristics

The shear test on full-scale masonry panels generally consists of a horizontal load applied at the top of the wall, which must be fixed to a rigid base. However, van Vliet [14] presents an inventory of in-plane shear experiments in masonry panels (mostly monotonic) and points out that both the boundary conditions in the upper part of the panel and how the horizontal forces are applied may vary. Table 1 chronologically presents some experimental setup types used in cyclic shear tests performed on full-scale elements.

Table 1. Experimental setup types used in cyclic shear tests.

References	Type of Experimental Setup	Description
[15]	Shear without external vertical load; free rotation; shear combined with bending.	A deformation-controlled horizontal cyclic loading was applied on a reinforced concrete beam at the top of the wall panels. The frame used to apply the load was not described.
[16]	Shear without external vertical load; rotation partially restrained; laterally distributed load.	The masonry panels were inside a steel frame, which was cyclic and quasi-statically loaded horizontally. The steel frame pillars, in theory, can transfer horizontal loads in a distributed way (non-uniformly) on the side of the wall.
[17,18]	Shear with external vertical load; rotation restrained; double bending.	The investigations were focused on the behavior of reinforced masonry panels under earthquake loading, and all carried out experiments using the same setup. Two vertical actuators acted to restrain rotation at the top of the walls, and a horizontal actuator applied forces at a rigid beam.
[19]	Shear with external vertical load; rotation restrained; double bending.	The vertical force was applied first, and the horizontal cyclic load was then applied, keeping the vertical jacks' valves closed. No rotation was theoretically possible, and the double-bending condition was present. As a consequence of the test mode, the vertical load increased together with the horizontal load, depending on the stiffness degradation. Tests were performed according to the Rilem Guidelines (1998). The test setup, however, had as a differential the fact that the top of the wall was attached to the underside of a reaction slab, while the horizontal load was applied to the reinforced concrete base on which the wall was built, which was located on a mobile platform. The vertical jacks were not installed on the top of the masonry, but below the mobile platform.
[20–24]	Shear with external vertical load; rotation restrained; double bending.	Frumento et al. [25] presented the interpretation of the results of shear tests on clay unit masonry walls carried out in different laboratories throughout Europe: ZAG—Ljubljana—Slovenia (ZAG), University of Dortmund—Germany (UD), University of Padua—Italy (UPD), UTCB—Bucharest—Romania (UTCB), and University of Pavia and EUCENTRE—Italy (UPV—EUC). In the case of cyclic lateral tests, the walls had been subjected to constant vertical load and cyclically acting horizontal loading. The horizontal load had been applied in the form of programmed displacements, cyclically imposed in both directions, with step-wise increased amplitudes up to the collapse of the specimens with different typologies and dimensions.
[26]	Shear with external vertical load; rotation restrained; double bending.	Cyclic shear tests were carried out on plain and carbon fiber polymers retrofitted masonry walls. The vertical (axial) force was kept constant during the test (control in force) and was uniformly distributed by a rigid steel beam of the pantograph. Due to the pantograph, the rotation of the upper beam was constrained, and the specimens were tested in double curvature. The cyclic lateral force was applied under constant axial load in the second step. The cyclic load was controlled in displacements due to the inelastic behavior envisaged for the tested specimens.

Table 1. *Cont.*

References	Type of Experimental Setup	Description
[27]	Shear with external vertical load; rotation restrained; double bending.	They performed in-plane cyclic shear tests of undressed double-leaf stone masonry panels. Two of the actuators apply an axial load to the specimen, while the third one is used to impose horizontal displacements to the top of the piers. Since a double bending configuration was chosen for all tests, the vertical rotation of the top steel beam was prevented by implementing a 'hybrid' control of the vertical actuators (they were forced to apply a constant total axial load and maintain the same vertical displacement). Specimens showing the same geometric configuration were tested for different levels of compression.
[28]	Shear without external vertical load; free rotation; shear combined with bending.	Quasi-static tests were conducted on full-scale specimens to confirm the ductile behavior of the proposed wall piers. The top and bottom ends of the reinforced concrete columns were connected by mechanical pins to a top steel girder and a strong floor. The top steel girder was driven by a 1000 kN actuator to impose the lateral drift cycles on the specimens.
[29]	In situ test; shear without external vertical load; shove test equipment set; shear-sliding behavior of brick masonry.	The shove test (ASTM Standard C1531) is an experimental technique aimed at studying the shear-sliding behavior of brick masonry (the jack is positioned within the masonry in places where brick units are removed). The work investigated the capability of the shove test in determining the shear strength parameters of brick masonries and highlighted the main advantages and disadvantages of the various testing methods.

As seen from Table 1, most experimental setups adopt the model with rotation restriction at the top and bottom, resulting in the double-bending condition. This configuration is interesting to understand the shear effects in situations with similar boundary conditions, such as multi-story buildings where structural masonry panels act confined between two slabs and under high compression, which reduces rotations. However, a limitation of this type of experimental setup is that the restriction to rotation at the top of the panel also prevents torsion, especially in panels with an asymmetric cross-section. In this way, the understanding of the integrated effect of combined torsion and shear may be impaired.

For situations involving low-height buildings (or for the upper floors of taller buildings), the vertical confinement effect of the panels tends to be significantly smaller. This is due to factors such as reduced panel compression, thin slabs, the eventual absence of a covering slab on the last floor, etc., which facilitate rotations at the top of the panels. In these cases, in addition to the bending effect becoming preponderant, the torsion effects can also be significant, especially in the case of panels with asymmetric cross-sections.

The SHS-Multirisk house model fits into this last category as it has only one floor; ideally, it does not have a covering slab, and the masonry panels up to 1 m wide and about 2.20 m high act close to the behavior of cantilever columns. In this way, we sought to develop a system without rotation restrictions at the top, which is believed to better reflect the real operational conditions of the house's panels under seismic loads. Thus, the tests reflect the shear behavior combined with bending and torsion (albeit partial) from applying the load on the axis that passes through the cross-section geometric center at the top of the wall.

2. Materials and Methods

2.1. The Specimens

As the designed system is not exclusive to the typology of the panels tested, the extensive experimental campaign will not be addressed in this paper, but the main results of two representative specimens tested (in-plane and out-of-plane shear) will be presented in Section 5, aiming to illustrate and analyze the main test system's outputs.

For the experimental campaign, 15 walls were constructed with a height near 2.30 m (~2.20 m for CEB masonry and ~10 cm for reinforced concrete beam at the top). The option for carrying out tests on full-scale specimens aimed at avoiding noise effects and distortions behavior between elements as reinforcement and masonry panels [12,30,31].

Twelve walls had a C-shaped cross-section (Figure 1) with 100 cm width and 12.5 cm thickness (six for in-plane cyclic shear tests and six for out-of-plane shear tests), and three had an L-shaped cross-section with 62.5 cm width and 25 cm thickness. They were constituted by soil–cement blocks (with two holes) in the proportion 8:1, vertical 10 mm diameter A500 steel bars (within five filled holes in C sections and within nine filled holes in L sections), horizontal 6 mm diameter A500 steel bars (in four 55 cm-spaced levels, starting from the top), and soil–cement mortar in the proportion 5:1. All of the specimens were built on a 60 cm height reinforced concrete base and designed with the same layout and materials.

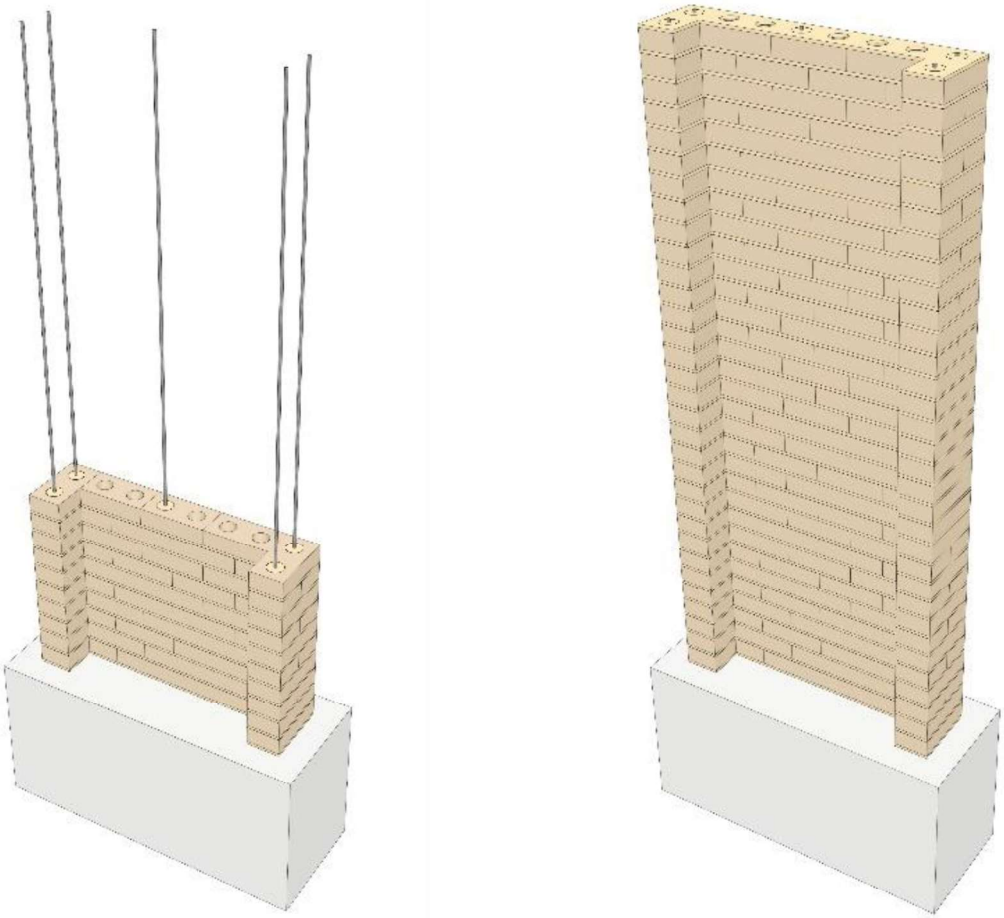

Figure 1. CEB C-panel and its vertical reinforcement within the filled holes.

2.2. The Designed Test Setup

A test system was designed and built to conduct cyclic shear tests on the full-scale walls, where the actuator imposes displacements on a simply-supported beam that, together with other elements, imposes displacements on the walls located in different positions (Figure 2).

The load cycle can be divided into four phases (Supplementary Materials). The first two correspond to the push configuration (displacements greater than the actuator half-stroke); the servo-actuator imposes positive displacements to the main beam, and the system imposes positive displacements to the wall specimen. While in the first part of the cycle, the displacements increase (Figure 3a), in the second part, they decrease (Figure 3b).

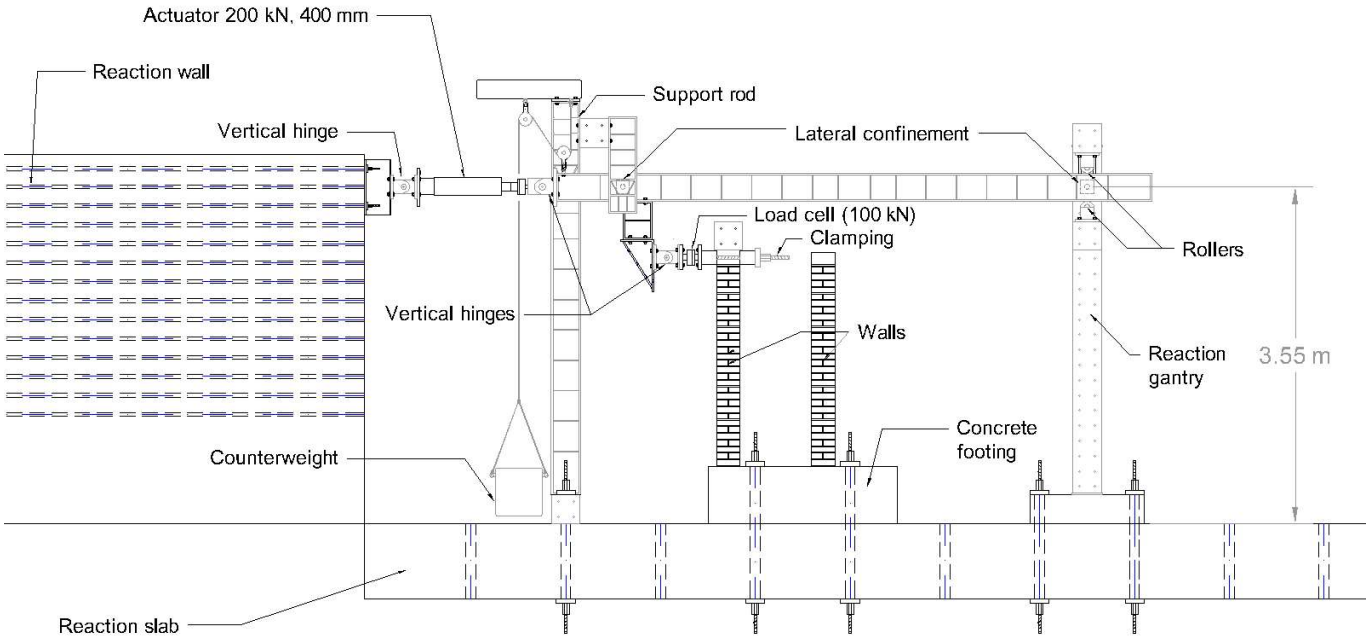

(**a**)

(**b**)

Figure 2. Cyclic shear test system for full-scale walls: (**a**) illustrating out-of-plane tests and (**b**) prepared for in-plane tests.

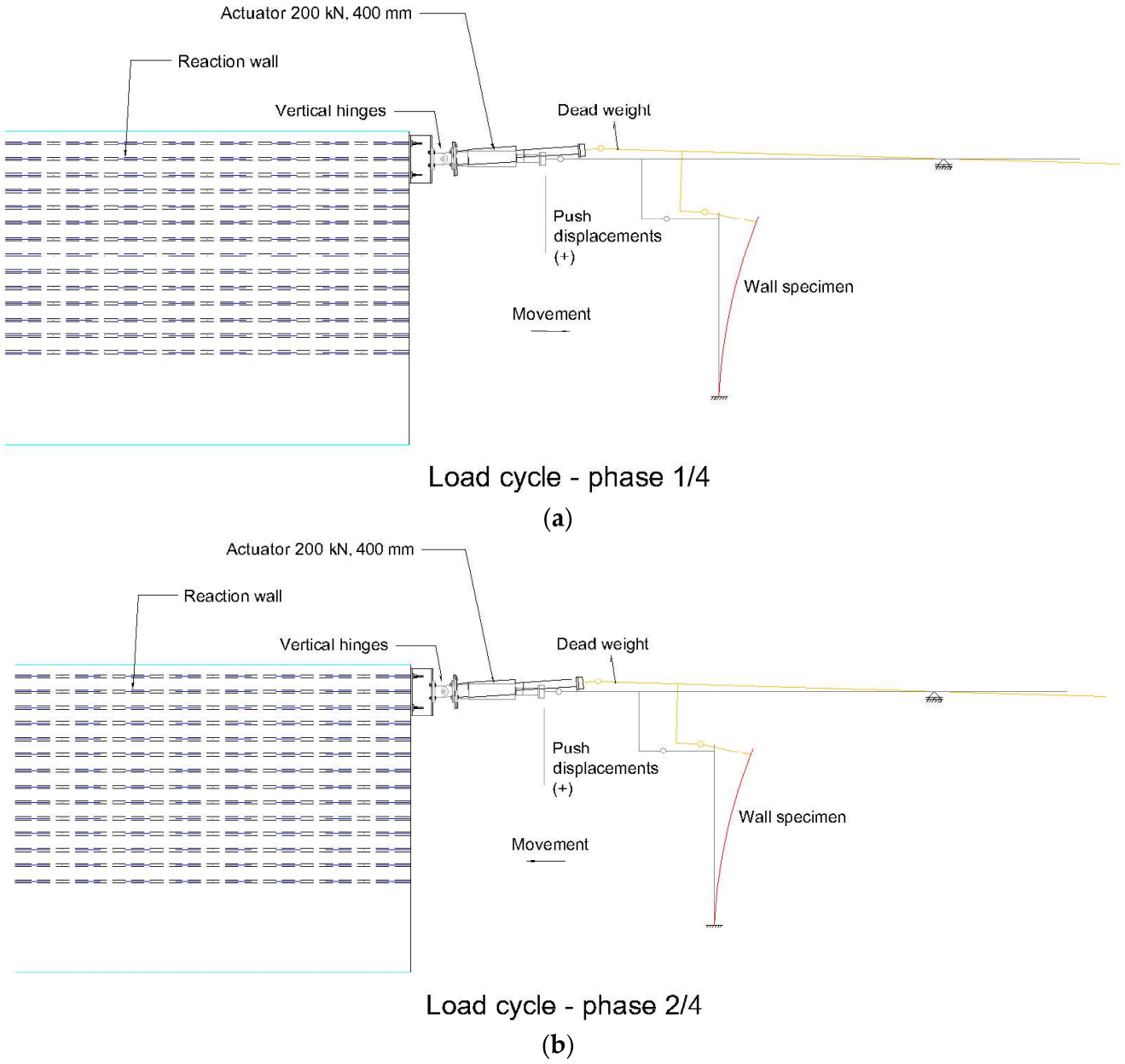

Figure 3. Test system operability under push configuration. (**a**) Displacements are increasing. (**b**) Displacements are decreasing.

The last two phases correspond to the pull configuration (displacements lesser than the actuator half-stroke); the servo-actuator imposes negative displacements to the main beam, and the system imposes negative displacements to the wall specimen. While in the third part of the cycle, the displacements increase in absolute value (Figure 4a), while in the fourth part, they decrease (Figure 4b).

Although only one specimen is tested at a time, Figure 5 illustrates the system positioned for testing a specific wall (the wall to be tested has overload elements at the top) among other walls constructed on the same footing. The walls to be tested under in-plane shear are shown in Figure 5a, and those to be tested under out-of-plane shear are shown in Figure 5b.

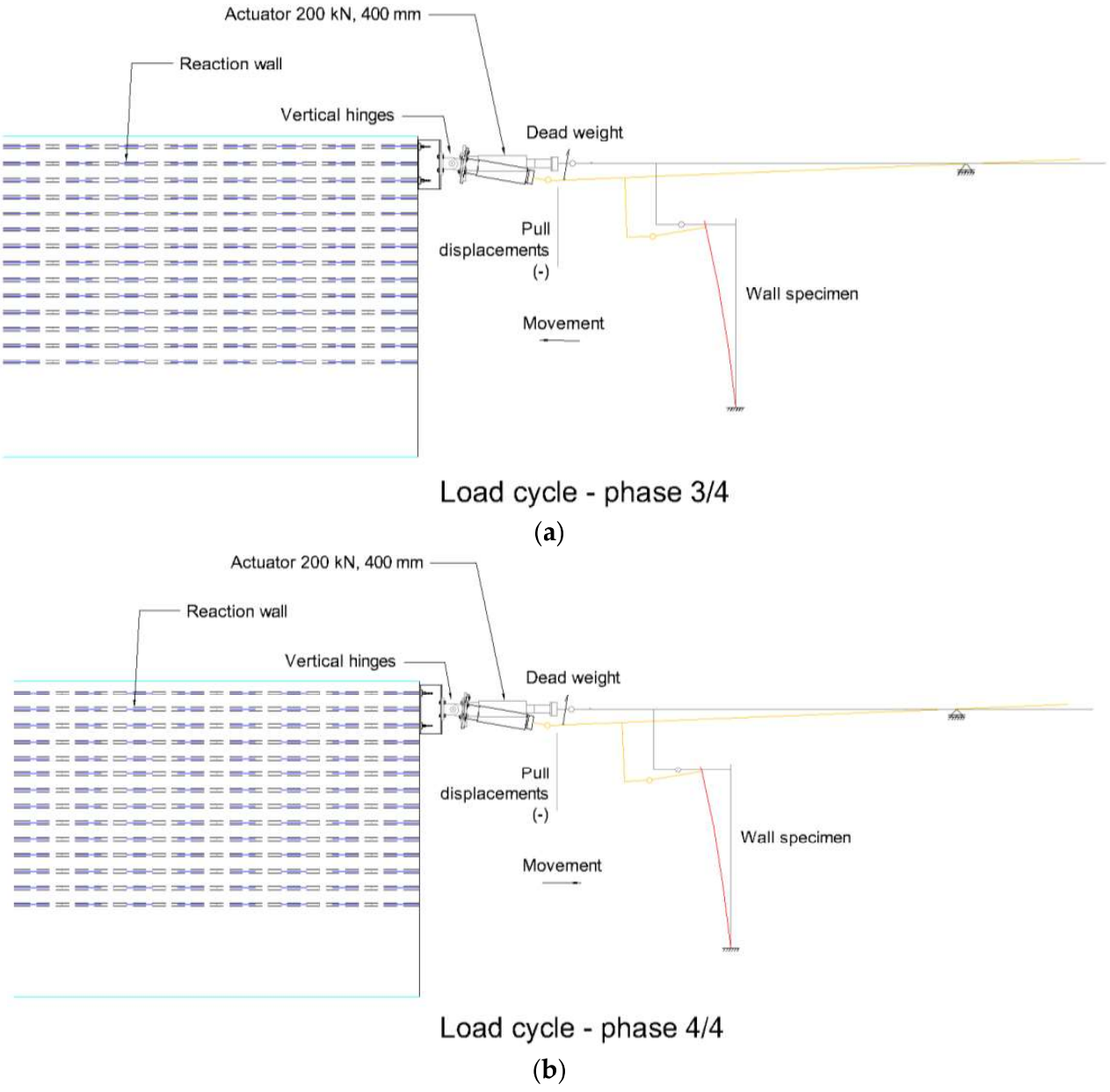

Figure 4. Test system operability under pull configuration. (**a**) Displacements are increasing (absolute values). (**b**) Displacements are decreasing (absolute values).

(**a**)

(**b**)

Figure 5. Wall specimens for cyclic shear tests: in-plane (**a**) and out-of-plane (**b**).

2.3. The Development Process

The test system, designed in the open-source framework, was ruled by the following guidelines:

- *Simplicity*. Through a structural arrangement that combined an actuator with basic structural systems (a reaction wall, a simply-supported beam, and a steel reaction gantry fixed in the base) and displacement transfer elements (connection pieces between the test beam and the specimen), an attempt was made to facilitate assembly and

reduce the complexity of potential unforeseen events. Vertical hinges were inserted to increase the degrees of freedom and to allow for the compatibility of rotations between the system components and the elements to be tested. A counterweight was inserted in the system close to the hinge connection between the actuator and the main test beam, seeking to facilitate the beam's vertical movement and consequently reduce the vertical shear force on the load cell positioned close to the wall.

- *Availability of components, equipment, and human resources*. In addition to environmental sustainability, an attempt was made to use the existing pieces and equipment in the UA's Civil Engineering Laboratory to save financial resources and reduce work time. Thus, acquiring and manufacturing new elements were carried out only when strictly necessary (it is estimated that nearly 95% of the parts available in the laboratory were used to construct the test system). The manufactured parts were basically connection plates to make different drilling modulations compatible. Adaptations in existing parts for hole enlargement (transformation of simple holes into oblong holes) were also made to accommodate adjustments of measures in the connection of the test system with the specimens. New elements were acquired to allow for the movement of concrete footings and wall specimens, such as roller skids and two-point load lifting systems. In addition, a base footing was built in reinforced concrete with plan dimensions of 2.00 m $\times$ 2.00 m with a height of 60 cm; this footing, together with two existing rectangular ones measuring 3.00 m $\times$ 2.00 m $\times$ 0.60 m each, allowed for the simultaneous construction of all 15 full scale wall specimens on the top of the footings.
- *Rationalization of available space*. The part allocated to structural activities corresponded to approximately 1/3 of the UA Civil Engineering Laboratory. In addition, considering the area occupied by other specimens awaiting tests, in addition to the unavailability of the spaces reserved for further experiments, the site available was approximately half of the area reserved for the structures, that is, near 60 m^2. In this way, the test system and the footings with the wall specimens were designed to be operated and moved within this area.
- *Scalability of tests in the available time*. Bearing in mind that the traditional shear test system contemplated only one wall per footing and the experimental program indicated the need to test 15 walls, different options for organizing the specimens to be tested were studied. In the first option, considering that the minimum life cycle time of a specimen was about two months (one week for construction, four weeks for curing, one week for instrumentation, one week for moving/testing/demolition, and one week for unforeseen/scheduling conflicts with other activities), the minimum time to carry out the work (disregarding the time to manufacture the blocks, transport, assembly of the test system, and recess/vacation periods) would be approximately 10 months [number of cycles (15 walls/3 footings available) $\times$ time per cycle (2 months) = 10 months]. In addition to the highly time-consuming feature, this configuration proved unfeasible due to the unavailability of external labor (masons) to construct the specimens intermittently for long periods. Considering the lack of space in the laboratory, the second option studied was to manufacture 13 footings and build the wall specimens outside the UA campus (at industrial facilities located about 18 km away). This alternative was discarded due to the possibility of the specimens suffering damage in transport. Finally, the third option (adopted) was to build all the specimens simultaneously in the laboratory on the three available footings (there were six C-shaped walls built on each rectangular footing, half for in-plane tests—Figure 3a—and half for out-of-plane tests—Figure 3b—, and three L-shaped walls over the square footing). This alternative made it possible to concentrate the construction services in well-defined periods, favored the supervision of the work, reduced the factors of constructive variability, shortened the work, and made the availability of specimens more flexible to meet the experiment's needs. In addition to allowing test logistics for the specimens by moving the footings in the laboratory work area, this option required adapting the test system to test the specimens in different

positions as the footing fixation on the reaction slab was very restrictive (drilling with 1 m modulation in both directions).

Considering the short time available (initially eight months, exceptionally extendable for up to four months) for designing and manufacturing the test system and for carrying out the shear tests on 15 full-scale wall specimens, it was decided to adopt a project management framework in Scrum mode, aligned with four main precepts of the Agile philosophy:

- Individuals and interactions are preferred over processes and tools;
- Working products are preferred over comprehensive documentation;
- Customer collaboration is preferred over contract negotiation;
- Responding to change is preferred over following a plan.

Scrum is a management framework considered lightweight, interactive, and incremental, used for developing and delivering new products, including those involving innovations [32]. Instead of a formal, sequential, and bureaucratic structure, the Scrum structure prioritizes the self-organization of small teams, where the main product is divided into well-defined parts developed and implemented in an interactive process organized in sprints, where the empirical practice is valued in conjunction with formal knowledge.

Three people constructed the 15 specimens over approximately four weeks between November and December 2021. The design of the test system started in January 2022, with the start of assembly in March 2022. The team tested and validated the successive assembly stages in fortnightly meetings, with daily sessions to discuss technical issues and routine unforeseen events. Disregarding the adjustment periods of the test system, vacation breaks, holidays, and other unforeseen circumstances, it is estimated that the complete test cycle of the 15 walls effectively lasted about four months, resulting in an average of eight consecutive days per sample. It should also be highlighted that the COVID-19 (COronaVIrus Disease of 2019) Pandemic marked 2021 and 2022, and that the non-renewal of the state of alert in Portugal only occurred at the end of September 2022.

2.4. The Experiment Execution Process

Once the main elements of the test system are assembled (base, loading, support, and load transfer subsystems, except for the transition elements) and the instrumentation subsystem is defined, the experiment execution process can be broken down into the following subprocesses: test preparation, testing the specimen, and demobilization. These processes are mapped in the flowchart below (Figure 6) and will be discussed in Section 4, aiming to better illustrate the system's operability.

2.5. Introducing the Numerical Investigation

A fundamental numerical investigation is presented in Section 5, using the main variables obtained from the shear test: displacements and forces at the servo-actuator and the top of the wall.

As the developed system is not exclusive to the walls tested in this experimental campaign, the numerical investigation aims to capture the main system's outputs in two representative test models: in-plane and out-of-plane shear (combined with bending).

As the acquisition system frequency was 20 Hz (20 measures obtained per second), it was necessary to run a programmed routine in the software Matlab version 2022b to reduce the noise and compile data to reduce the file size. The noise reduction was treated by applying the moving average function to five subsequent values. The compiling function adopts a simple mean as a representative value of each discrete interval of five registers. This makes it possible to reduce the data four times (equivalent to 5 Hz) and maintain representativity.

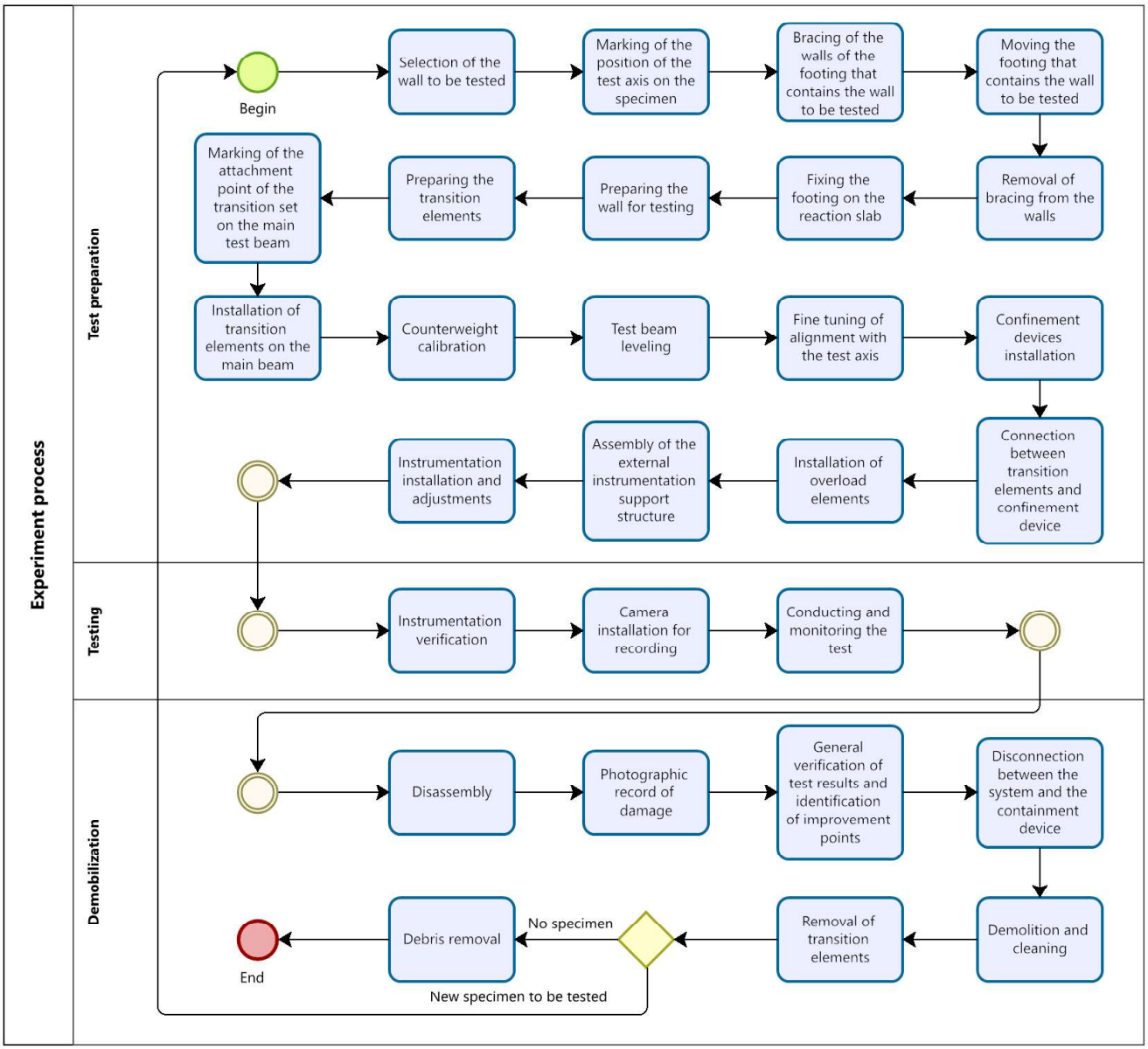

Figure 6. Flowchart containing the experiment execution process, subprocesses, and activities.

After obtaining the reduced data file, data treatment continued using electronic worksheets. Firstly, all of the sensors were plotted with time to verify the occurrence of any anomaly and then limit the range of useful quality data. After this stage, the forces-displacements diagrams of two representative specimens tested were plotted and discussed in the sequence.

3. Test Setup Description

The test system was divided into seven subsystems with specific functions:

(1) *Base subsystem*: is responsible for providing rigid bases for fixing the main elements participating in the test system: servo-actuator, reaction gantry, support rod, and specimens;
(2) *Loading subsystem*: is responsible for imposing loads on the test system in a controlled manner (in the case under study, displacement control);
(3) *Support subsystem*: is responsible for providing support to the main test beam to restrict undesirable displacements (torsion rotations and vertical displacements near

the gantry) and allow for the desired movements (vertical movement outside the gantry, horizontal direction, and rotation in the test plane);

(4) *Load transfer subsystem*: is responsible for transferring displacements and forces from the actuator to the specimen, even if not completely, due to the allowed rotations and the geometry of the system;

(5) *Logistics subsystem*: is responsible for allowing the transport of heavy loads (system components and test specimens), both for assembly and for operation;

(6) *Security subsystem*: devices capable of reducing risks during system assembly and operation;

(7) *Instrumentation subsystem*: allows for monitoring and recording of displacements on the specimens, base footings, main beam, and also to determine the force transferred to the testing wall, aiming to control key parameters during the test and allow the subsequent data analysis.

3.1. Base Subsystem

This subsystem comprises the following elements (and their respective functions): reaction wall (serving as a rigid support for the servo-actuator), reaction slab (serving as a rigid support for the concrete footings, the steel reaction gantry and the support rod), and reinforced concrete footings (acting as the basis for the specimens to be tested).

The actuator was indirectly connected to the reaction wall, considered perfectly rigid, using a set of metallic plates and a vertical hinge (Figure 7a); the connection between the main test beam and the actuator arm was also made using metal plates and a vertical hinge, allowing the system to operate with a greater number of degrees of freedom and thus reducing the appearance of forces and moments or movement incompatibilities due to restrictions of displacements.

(**a**) (**b**)

Figure 7. (**a**) Servo-actuator connection to the reaction wall; (**b**) fixing the footing on the reaction slab.

The walls were built on rigid reinforced concrete footings 60 cm high, fixed at four points against the reaction slab through tensioned steel bars with a jack pressure of near 150 bars (Figure 7b). To allow for the lifting and transport of these elements, each footing had four horizontal handles made of 20 mm diameter steel bars anchored in the confined concrete.

The concrete footings with the constructed specimens were submitted to translational motions in both directions and rotation in the plane of the reaction slab so that the walls' distances relative to the reaction wall were relatively close in different configurations, seeking to avoid sudden variations in the test system outputs.

The base of the counterweight support rod was fixed to the reaction slab, similar to the reaction gantry (Figure 8a). The gantry was fixed to the floor using a set of beams and steel cubes compressed against the reaction slab employing tensioned steel bars with a jack pressure of approximately 380 bars (Figure 8b). With minor adaptations, the support reac-

tion gantry was later used in the mechanical characterization of the reinforced compressed earth blocks masonry [33].

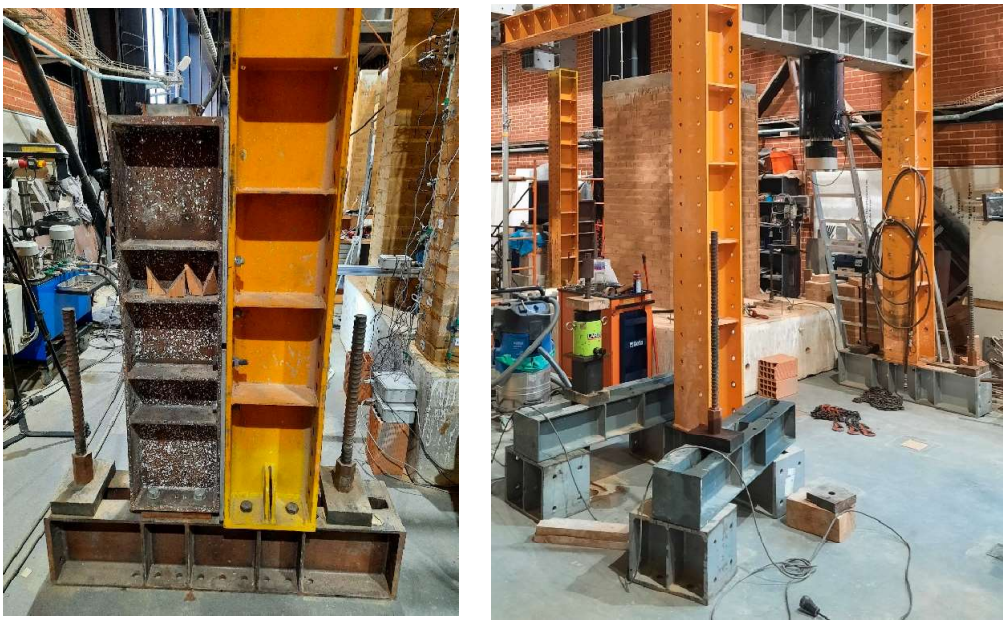

(**a**) (**b**)

Figure 8. (**a**) Fixing the counterweight support rod to the reaction slab; (**b**) fixing the gantry to the reaction slab.

3.2. Loading Subsystem

This subsystem comprises the following elements: a servo-actuator (Figure 9, serving as an active loading device), a pressure control unit, and the module with an acquisition system and servo-actuator control software.

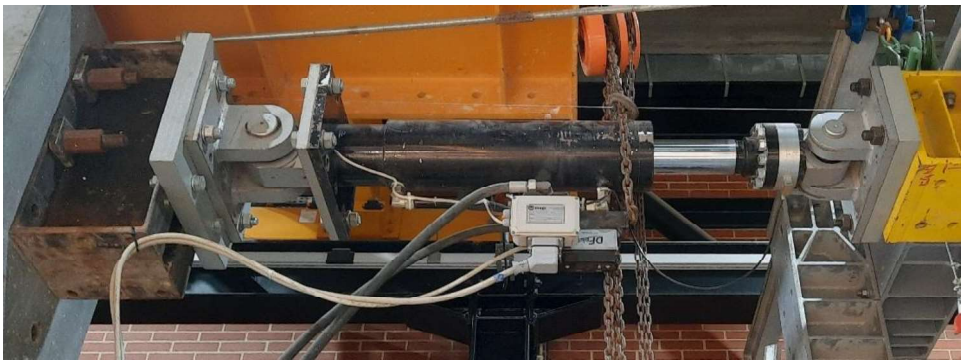

Figure 9. Servo-actuator with 200 kN of capacity and 400 mm stroke.

By applying forces towards the servo-actuator, this subsystem is responsible for imposing displacements in a controlled manner on the main test beam, which mobilizes other connection elements until, finally, the wall is requested at the top.

The servo-actuator had a stroke of 400 mm and a load cell with a capacity of 200 kN both in tension and in compression. The pressure control unit provides (i) the hydraulic system of the servo-actuator with the necessary pressure to induce the displacements law (load protocol) and the (ii) electric current to the module and acquisition system. The pressure control unit also provides electric protection to all systems against current surges or power failure, ensuring that no data are lost.

The control software allowed for programming the displacement law, imposing the displacements at constant speeds, at the end of the actuator and sufficiently slowly, allowing for disregarding the effects of inertial forces, in the following stages:

- For in-plane shear tests: 0.1 mm/s (up to 5 mm) and 0.5 mm/s (from 5 mm on);
- For out-of-plane shear tests: 0.1 mm/s (up to 5 mm), 0.5 mm/s (from 5 mm to 7.5 mm), and 1.0 mm/s (from 7.5 mm on).

3.3. Support Subsystem

This subsystem comprises the following elements (and their respective functions): reaction gantry (serving as a simple support for the loading transfer subsystem), counterweight set (acting as a simple support for the main test beam), support rod (serving as support for the counterweight set and the displacement restriction devices), and displacement restriction devices (serving as lateral support for the main test beam).

The gantry was built with stiffened H 300 × 300 steel beams, with modulated holes every 16 cm in the pillars and the two beams installed jointly in the upper part (Figure 10a). The bases were fixed as described in Section 3.1, and a set of unidirectional rollers was installed at the top of the upper beam to function as a simple support for the lower face of the main test beam. This configuration was sufficient for out-of-plane shear tests involving small resistive horizontal forces. However, for the in-plane tests where the resistive forces were, on average, five times higher than the out-of-plane forces, it was also necessary to install a beam with another set of unidirectional rollers on the top part of the test beam (Figure 10b,c), to prevent the detachment of the beam from the gantry and rotation due to torsion at this point. Steel cubes were also installed on the upper part, where two systems of spherical rollers were laterally fixed to prevent horizontal displacements of the main beam at this point (Figure 10b,c). At the same time, metal plates were welded to the test beam to allow it to slide freely on the spherical rollers.

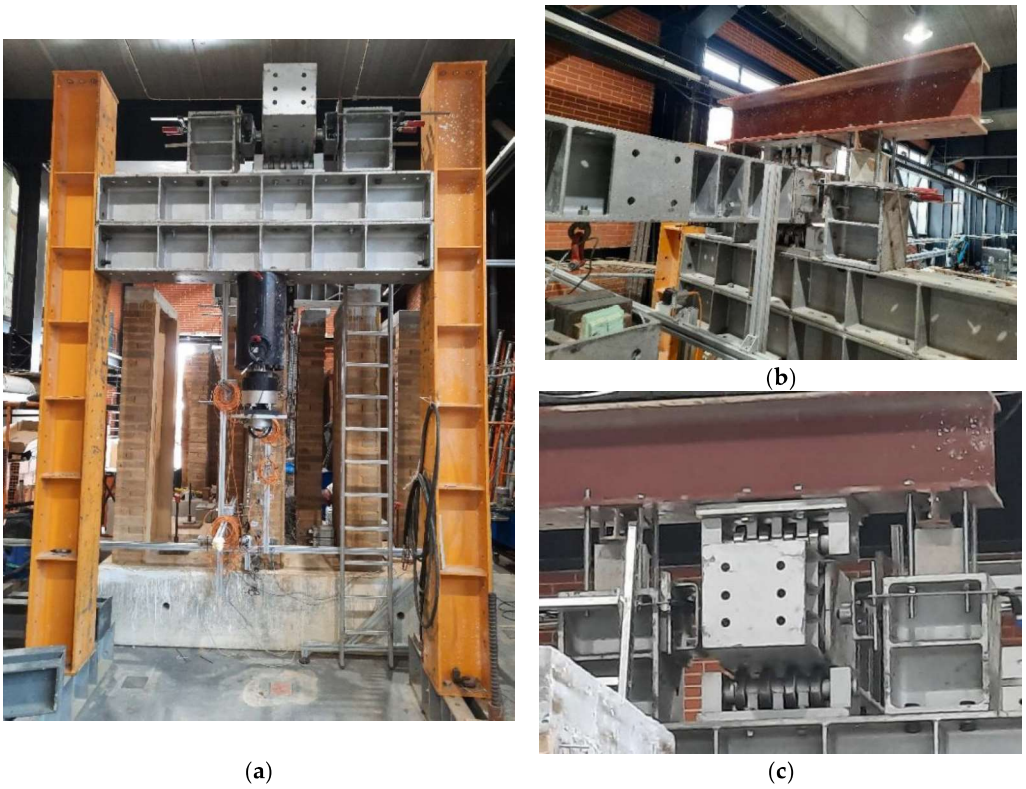

(**a**) (**b**) (**c**)

Figure 10. (**a**) Reaction gantry. (**b**,**c**) Details of the set of rollers for vertical, horizontal, and torsional support.

A suspension cable linked to a constant mass counterweight was installed and connected to a pulley system (Figure 11), aiming to support a loading transfer subsystem near the servo-actuator and simultaneously allowing movement at this point. This device could balance the loading transfer subsystem in the initial position and reduce the incidence of shear forces on the actuator and the shear forces next to the load cell installed close to the wall specimens. Once the counterweight system was installed and calibrated, the vertical movement of the test beam could be tested manually by just one person, even with some effort attributed to the friction and inertial forces of the system. In addition, the pulley system allowed the mass needed to balance the counterweight to be approximately 57% of the mass at the point of suspension, facilitating calibration and the operation of the loading, support, and load transfer subsystems.

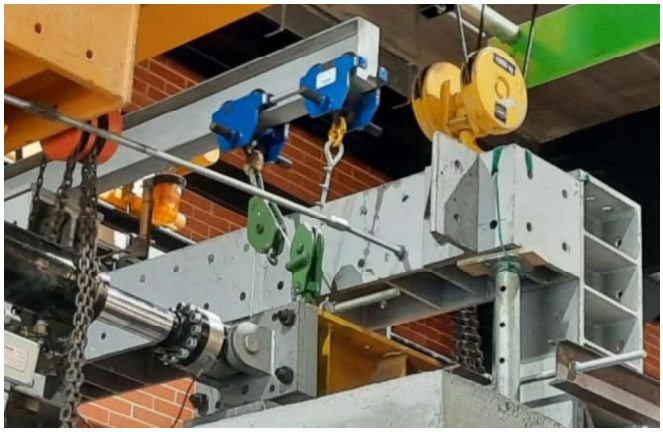

(**a**)

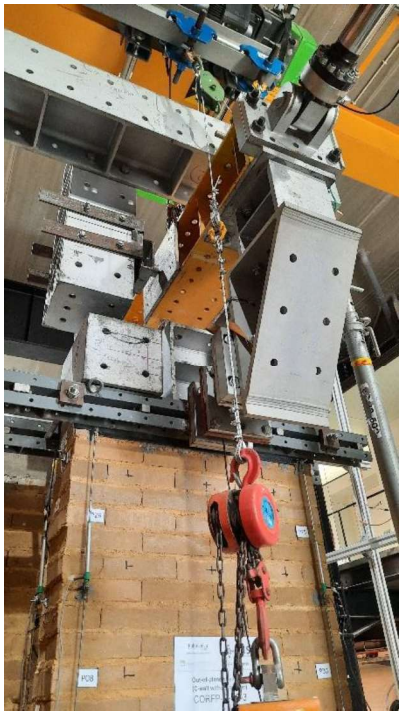

(**b**)

(**c**)

Figure 11. (**a**) Detail of the pulleys and trolleys set. (**b**) Suspension of the counterweight on the pulleys set with steel cable. (**c**) Suspended counterweight.

The support rod was a structure created with a double function: to support the elements of the counterweight assembly and to prevent lateral movements of the test beam

close to the suspension point (Figure 12). To support the counterweight set, a transverse I-shaped steel beam was fixed at the top of the rod, where two hand trolleys with a capacity of 1 ton each were installed. The end of the steel cable was attached to one fixed trolley, while one of the pulleys was attached to the other. The other pulley was installed inverted on a bar attached to the test beam. As this installation of pulleys took place using eye nuts, rotation was allowed. Plates with double spherical rollers were installed in vertical H 300 × 300 steel beams with about 1 m in height on both sides, aiming to restrict the beam's movement near the suspension point (torsion rotations and horizontal out-of-plane displacements). At the same time, steel plates were welded to the sides of the beam, allowing it to slide freely on the spherical rollers. It is necessary that the half stroke of the actuator coincides with the axis of the lateral confinement plates, over which the rollers will slide. The length of the plates must be equal to or greater than the stroke of the actuator, which will allow the rollers to act within the plates' limits during the test. The vertical pieces were fixed to an H 300 × 300 cantilever beam, which was fixed to a column composed of H 300 × 300 pieces stiffened in the first 2 m along the base. The base, in turn, was fixed to the reaction slab, as described in Section 3.1.

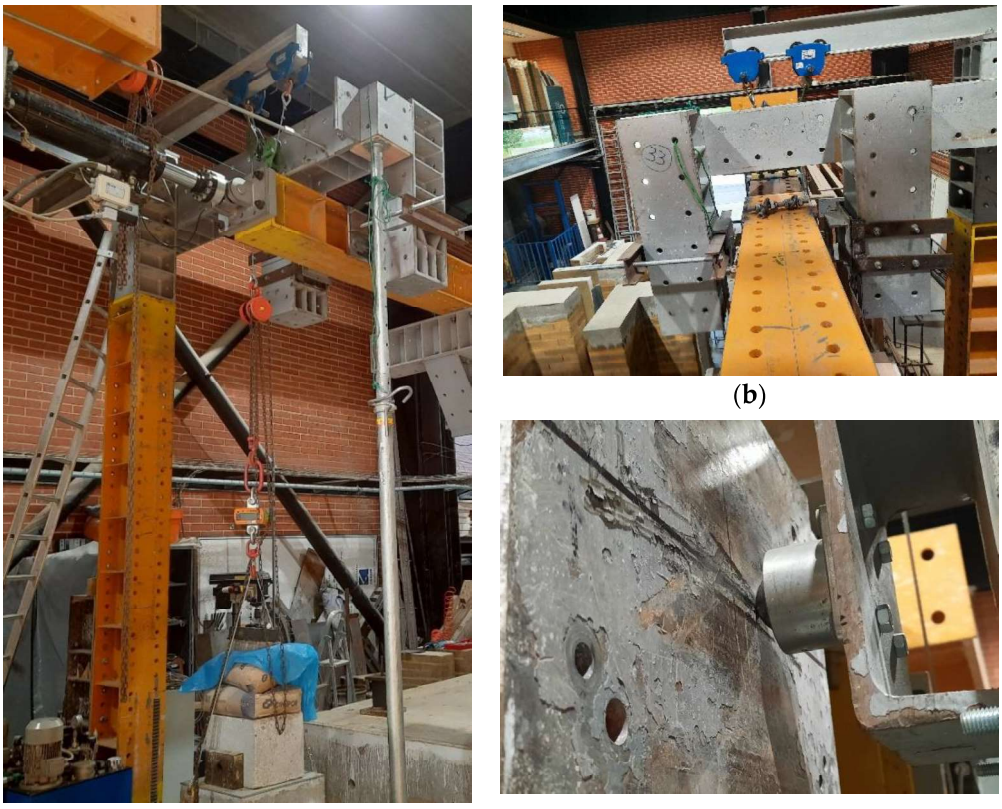

(**a**) (**b**) (**c**)

Figure 12. (**a**) Counterweight support rod. (**b**,**c**) Lateral support rollers.

3.4. Load Transfer Subsystem

This subsystem comprises the following elements (and their respective functions): main beam (transferring displacements from the actuator to the other passive loading elements), hinges (allowing rotations and then increasing the system's degree of freedom), and other high resistance metallic elements (transferring forces and displacements to the wall specimens). To obtain the horizontal forces and displacements at the top of the wall (the main objective of the cyclic shear test), a load cell with a capacity of 100 kN was inserted between the hinge and the wall. Although the load is applied at the confinement devices plates, which transfer it to the concrete beam's surface in a distributed manner, it is registered as a concentrated load as the cell is located at the load axis. The displacement

transducers were fixed in an external rigid aluminum structure independent of the specimen and to the concrete footing foundation of the specimens.

As already mentioned, the purpose of the hinges was to allow the system to operate with a greater number of degrees of freedom and then reduce the interference of forces and moments at the specimens and prevent movement incompatibilities due to displacement restrictions. Thus, hinges were installed at three points (Figure 13): the connection between the actuator and the wall, the connection between the actuator and the main test beam, and the connection between the wall and the vertical transition element (steel triangle). While the first two hinges provide the possibility of rotation on the main test beam and thus reduce the vertical forces on the wall and the load cell, the hinge next to the specimen allows the wall rotations to occur relatively independently of the rotations of the load cell, as the transfer of momentum from the test system to the wall is prevented.

(**a**) (**b**) (**c**)

Figure 13. Details of the hinges positioned before the servo-actuator (**a**), after the servo-actuator (**b**), and next to the specimen (**c**).

The main test beam comprised stiffened H 300 × 300 steel pieces with high flexural and torsion rigidity. These elements allowed the system to function within the test plan, together with the displacement restriction devices positioned on the gantry and the support rod (Figure 14). This beam, for which the axis was aligned with the reaction wall and with the servo-actuator axes, was leveled before connecting the test system to the specimen and was positioned at an elevation of about 60 cm above the top of the walls, so as not to interfere with the other walls built on the same footing.

Figure 14. Main test beam.

As the main beam had holes every 8 cm, a set of transition elements was installed between the main beam and the wall to be tested (Figure 15). These elements were connected to the lower table of the main beam and descended vertically until it was possible

to apply the load at an approximate height of 2.20 m from the footings (in the direction of the middle horizontal section of the reinforced concrete beam built at the top of the wall). The counterweight calibration was performed after installing the transition elements and before connecting the test system to the specimen.

(**a**) (**b**)

Figure 15. Detail of transition elements for in-plane (**a**) and out-of-plane (**b**) configurations.

The load application point was in line with the geometric center of the wall cross-section, aiming to portray the closest behavior in a seismic context, in which the forces mobilize the vertical axis that passes through the centers of mass of the rows, considered as a homogeneous material. Adjustments for applying loads at the desired point and eliminating gaps between the test system and the specimens located in different positions on the footings were achieved through the following mechanisms:

- Position adjustments along the main test axis. These adjustments were basically made in three ways: moving the footings along the test axis (multiple adjustments of 1 m $\pm$ 4 cm, the latter due to gaps in the steel bars in the holes of the footings/reaction slab), changes in the fixing position of the transition elements along the hole in the main beam (adjustments multiple of 8 cm), and fine adjustments in the actuator (less than 8 cm).
- Adjustments in the direction orthogonal to the test plane. At first, the adjustments were possible through the following alternatives: lateral movement of the footings (multiple adjustments of 1 m $\pm$ 4 cm, the latter due to gaps in the steel bars in the holes of the footings/reaction slab) and execution of oblong holes in the plates for fixing the system to the wall (fine adjustments of up to 2 cm). The walls tested in out-of-plane shear were built with axes in positions of multiples of approximately 1 m and aligned with the holes in the footings. The mentioned alternatives were sufficient to reduce the eccentricity to a maximum of 1.5 cm in sections 100 cm wide. As for the walls tested in the plane of the wall, it was necessary to increase the possibilities of lateral displacement, considering that they were built with their geometric centers in positions of multiples of 16 cm. The following measures were additionally thought out to reach this objective: the installation of a metallic beam transversal to the main beam (Figure 15a), allowing the fixation of the triangular vertical transition element in multiple positions of 16 cm (up to the limit of 48 cm of eccentricity to the main test axis), and execution of oblong holes in the triangular transition element (at the top and on the side, allowing fine adjustments of up to 4 cm).

Confinement devices were designed at the top of the wall for in-plane (Figure 16a) and out-of-plane (Figure 16c) tests involving metal profiles, steel plates, and threaded bars. These elements were installed on the two faces of the specimen orthogonal to the test plane. Then, they were tensioned against each other so that the specimen could be mobilized in both directions (positive and negative displacements of the actuator) without gaps. In both contact interfaces of these elements with the wall, rubbers with about 5 mm thickness were inserted, aiming at a better uniformity of the contact surface.

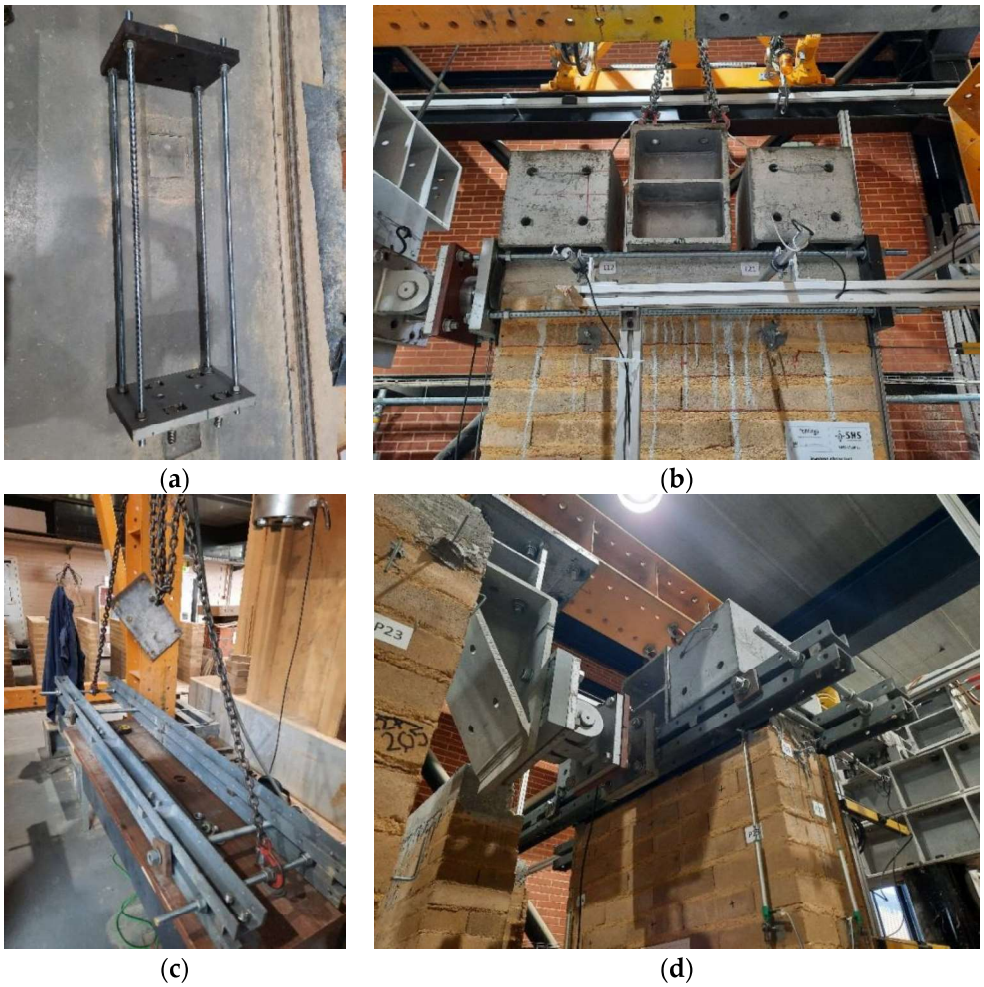

Figure 16. Clamping devices for the top of the walls and coupling in the test system: in-plane (**a**,**b**) and out-of-plane (**c**,**d**).

3.5. Logistics Subsystem

This subsystem is made up of the following elements: pallet truck (for lifting small loads), overhead crane (for lifting high loads), load spreader set (helping to lift the footings), and roller skids (to move the concrete footings in the horizontal plane).

For the conventional transport of loads, the laboratory had an overhead crane with a load lifting system (up to 10 tons), a hydraulic manual pallet truck (for loads of up to 2 tons), and manual hand trucks for small loads (up to about 250 kg). In addition, auxiliary devices such as straps, chains, eyebolts, and hooks also made up the collection of parts for these purposes.

However, the existing devices were not enough to move the reinforced concrete footings with the walls, and it was necessary to provide the following complementary elements:

- Spreader set for general cargo with a capacity of 10 tons (Figure 17a). This system had, in the upper part, a sling with two branches on chains connected to a square tubular steel profile in a triangular geometry arrangement, and in the lower part, it was composed of two chains with self-locking hooks for direct coupling to the lifting points of the footings. In this way, it was possible to install roller skids under the footings that would be moved.
- Heavy transport roller skids, with a capacity of 3 tons each. Four roller skids were purchased, and two more were temporarily provided by the UA Mechanical Engineering Laboratory. With a total capacity of 18 tons, these skids would initially allow for the movement of an entire large footing (full estimated load of 16 tons, including the

six walls). However, it was found that it was possible (and more efficient) to move each footing with only three skids positioned on one side of the shoe, and, on the other side, the crane itself associated with the spreader assembly was able to function as support and induce movement of the footings, both in straight displacements and in rotation (Figure 17b).

(**a**) (**b**)

Figure 17. (**a**) Load spreader assembly. (**b**) Movement of the footing with specimens, with the help of roller skids, load spreader assembly, and overhead crane.

Steel plates with the same height as the skids were also used as temporary leveling shims while the footings were waiting for movement. These shims also allowed the roller skids installation process to be carried out in two stages, avoiding greater demands on the walls during this operation. An attempt was also made to brace nearby walls to reduce relative displacements during the concrete footing movement, especially when the walls had already been tested and, thus, had reduced rigidity.

3.6. Security Subsystem: Security Devices

Safety devices were designed to act on the following elements (Figure 18) to increase the system safety level: servo-actuator, test beam, and specimen.

Next to the reaction wall, a manual hoist attached to a support beam immediately above the actuator was inserted so that the hoist chains involved the actuator body with some clearance; this allowed rotations of this equipment, but within certain safety limits.

Considering the high loads involved, the test system was designed to have one of its sides fully supported (in this case, by the gantry) for safety reasons. As mentioned, lateral restraints with spherical rollers and steel plates were inserted at two points (next to the gantry and close to the connection point of the counterweight cable. During the tests, care was taken to position the overhead crane connected to a possible lifting point of the test beam with some clearance capable of allowing movement within certain limits.

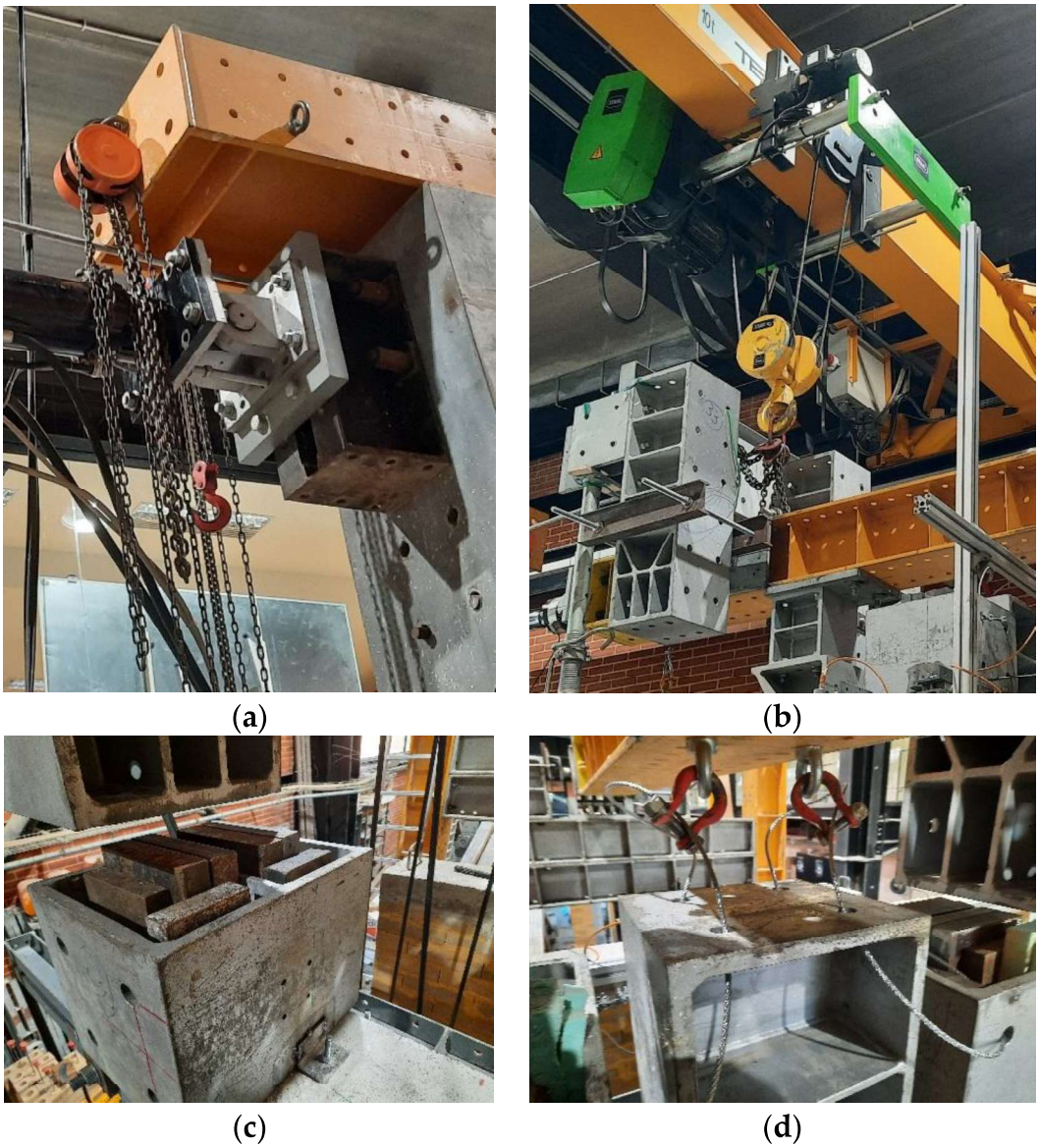

Figure 18. Details of the safety devices on the actuator (**a**) on the main beam (**b**) and on the specimen (**c**,**d**).

The specimen safety was ensured through the mechanical fixation of the overload elements in the reinforced concrete beam with structural bolts. The overload elements, in turn, were connected with steel cables to eyebolts attached to the main test beam to prevent the wall fallig.

In addition, the system operators monitored the entire test in person, who could interrupt the system at any time considered critical for safety.

3.7. Instrumentation Subsystem

This subsystem comprises the instrumentation used in the wall specimens (Figure 19), footings and main beam, the load cell at the top of the wall level, and the data acquisition system. The servo-actuator (only one is necessary for the proposed setup configuration) provides measures of displacements and forces.

In each situation, this subsystem must assume a very peculiar configuration depending on the specimen to be tested, the type of test, the key variables to be known and analyzed (forces and displacements at interest points, mainly), the surroundings of the wall to be tested, the variables necessary to be monitored for safety reasons, the reduction in noise

and uncertainties, among others, so the information presented below is merely illustrative of the case under study.

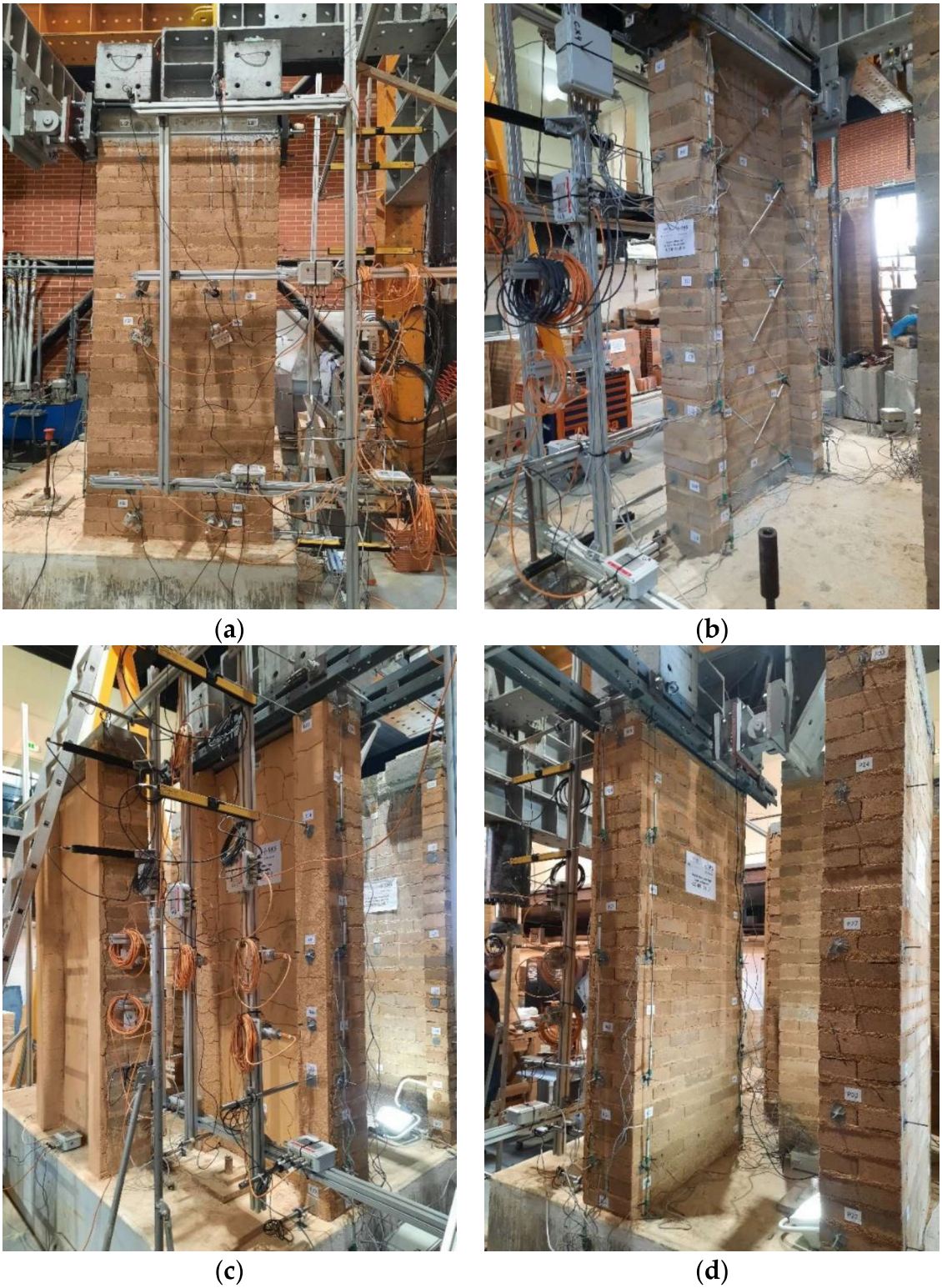

Figure 19. Instrumentation of the specimens in in-plane (**a**,**b**) and out-of-plane (**c**,**d**) configurations.

In the present experiment, instrumentation with external displacement transducers fixed to an independent rigid aluminum support structure was performed to capture both in-plane and out-of-plane displacements of the walls, including torsional rotations. External

sensors were also installed near the base of the specimen (to capture base displacements in the direction of the main test axis) and at three points of the base footings, seeking to capture unforeseen displacements. In addition, sensors fixed to the panels were installed in four parts along the height, aiming to find the deformations at the walls' reinforcements.

Sensors were also installed to capture horizontal displacements and rotations of the footing and to capture vertical displacements of the main test beam.

Five types of sensors were used: (i) LVDT's (Linear Variable Displacement Transducer) with ranges of 10, 25, 100, and 250 mm, with sensitivity of 1×10^{-3} mm; (ii) Rectilinear Displacement Transducer (Gefran) with ranges of 25, 50, and 100 mm, with sensitivity of 1×10^{-4} mm; (iii) Inductive Linear Position sensors with a range of 400 mm and sensitivity of 1×10^{-3} mm; (iv) Draw Wire Position sensors with ranges of 500 and 750 mm with sensitivity of 1×10^{-6} mm; and (v) a DSCC pancake load cell/low profile force sensor with both a tension and compression capacity of 100 kN.

It is important to highlight that for the principal test output analysis (performed in Section 5), only data from the load cells and the displacements at the servo-actuator and the top of the wall are necessary. However, sensors at the top and transversal to the wall help capture torsion rotations. These measures may be required (especially when the cross-section is asymmetric to the test axis) for obtaining the force component at the load cell and the component of the displacements parallel to the test axis. However, in cases where torsional behavior only significantly manifests for high displacements, this correction may be negligible.

The sensor positioning is very particular for each wall design and for points of interest that one wants to investigate. Although this paper does not aim to address the whole sensor positioning at the specimen, it is recommended that one considers some recent advances in sensor placement (i.e., sub-clustering strategy and considering multi-source uncertainties), mainly when the number of sensors is restricted [34,35]. Recent progress in the uncertainty theory and optimal control methods can be found in [36,37].

In the present study, two sensors were positioned to register the displacements at the top of the wall, which is considered a key variable, to provide redundancy. This measure was necessary to reduce the uncertainties as the data from two sensors could be compared and validated. The location of these sensors was not the same, aiming to reduce the possibility of problems due to some intercurrence at the elements to which the sensors are fixed (i.e., the concrete beam eventually could detach from the wall, and then both measures would be discarded if the sensors were at the same level). Thus, one of the sensors was fixed at the level of the axis of the concrete beam, and the other was set at the axis that passed through the last row of the wall. However, as the displacements in the test direction are generally proportional to the height of the sensor position related to the top of the base footing, the data from the lower position sensor have to be linearly projected to the level of the concrete beam axis. The two sensors were relatively near each other (nearly 20 cm), so the linear projection could be performed without losing significant precision.

The position of the load cell at the top of the wall (always perpendicular to it) also aimed at reducing uncertainties regarding the system rotations once it provides a direct measure of this critical variable, increasing reliability. Other sensors were positioned to minimize uncertainties, as their variables could be used to adjust the measurements obtained at the interest points. This is the case of the footing and wall base sensors, which monitor secondary movements that may affect the measures of the main sensors.

4. Experiment Execution Process Detailing

4.1. Test Preparation

The test preparation process can be broken down into the following activities: selection of the wall to be tested, marking the position of the test axis on the specimen, bracing the walls for transportation, moving the concrete footing containing the wall to be tested, removing the bracing from the walls, fixing the footing on the reaction slab, preparing the wall for testing, preparation of transition elements, marking the attachment point of the

transition set on the main test beam, installation of the transition elements on the main beam, counterweight calibration, test beam leveling, fine-tuning of alignment with the test axis, confinement devices installation, connection between the transition elements and the confinement device, installation of overload elements, assembly of the external instrumentation support structure, and instrumentation installation and adjustments.

4.1.1. Selection of the Wall to Be Tested

As the test is carried out on one wall at a time, it is necessary to determine the specimen test order based on criteria such as experimental planning, ease of access to the wall, space available for system operation, type and age of the specimens, interference with other activities, and priority for obtaining results, among others. The choice of the wall to be tested will determine the route for moving the concrete footing, aiming at aligning the specimen with the main test plan. It is important to point out that the main test plane does not necessarily coincide with the axis of the reaction wall, but it is a plane parallel to this axis that passes through the axis of the element that transfers the load to the wall; in the present study, this means the axis of the hinge located close to the wall.

4.1.2. Marking the Position of the Test Axis on the Specimen

The definition of the specimen's test axis must be based on what information is necessary to understand the wall's behavior. Among the possibilities for positioning the test axis at the wall, two stand out: the axis that passes through the geometric center of the cross-section (in this case, there will be torsion) and the axis that passes through the wall's torsion center (in case one wants to reduce the torsion effect as much as possible). In this research example, as the aim is to investigate the behavior of reinforced masonry CEB panels under seismic situations, the test axis was defined from the geometric center of the specimen's cross-section. As the seismic actions mobilize the rows' mass center, and the geometric center of the ideal cross-section of homogeneous material is very close to the mass center, it is expected that this configuration is adequate to apply the test results in a future seismic analysis. For standardization purposes, it is recommended that this marking be made on the specimen's base as constructive defects may lead to random deviations from the plumb line in the upper part of the walls. These deviations must be registered before the test begins so that they can be appropriately considered in the data analysis.

4.1.3. Bracing the Walls for Transportation

Before moving the concrete footing, it is recommended that the walls be braced in pairs to increase the rigidity of the set and minimize displacements and damage during movement. In the example mentioned in this article, bracing was done with metal struts in an 'X' shape and lashing straps at the top; there was no visible damage to the walls after moving.

4.1.4. Moving the Concrete Footing Containing the Wall to Be Tested

This movement is done in three steps: upward vertical movement to install the load skids, horizontal rotation and translation, and downward vertical movement to remove the load skids. The motion must be carried out in continuous stages and at low speed, minimizing sudden interruptions caused by the overhead crane activation. The movement must be carried out to position the holes in the concrete footing aligned with the holes in the reaction slab in a position that best approximates the test plane to the wall's test axis.

4.1.5. Removing the Bracing from the Walls

After positioning the concrete footing, the bracing of the walls can be removed and thus free up space for work and movement of people.

4.1.6. Fixing the Footing on the Reaction Slab

The concrete footing is fixed at four points against the reaction slab through tensioned steel bars with a jack pressure of approximately 150 bars.

4.1.7. Preparing the Wall for Testing

After defining the sensors and their positions, the wall is prepared for the installation of the sensors, which, in this case, were basically of four types: After marking the positions of the sensors of types (ii), (iii), and (iv), drilling the wall, and vacuuming the powdery material, the 5 mm threaded rods were installed with epoxy. In places where type (i) sensors were used, acrylic plates glued with epoxy were installed. On the upper part of the concrete beam, the positions of the overload elements fixing points are marked and drilled, followed by dust aspiration and by the installation of steel anchor bolts.

4.1.8. Preparation of Transition Elements

The transition element from the load transfer subsystem (steel beam transversal to the main beam, metallic triangle, plates, and hinge with load cell) must be prepared and preferably adjusted on the ground for safety reasons. In addition, it is recommended that this subsystem be balanced with the overhead crane connected to the point that will be fixed to the main test beam by inserting metal plates on the opposite side to the side where the triangle is positioned. This measure prevents the transition elements from causing torsion in the main beam in the initial test position.

4.1.9. Marking the Attachment Point of the Transition Set on the Main Test Beam

Considering that the actuator is in the half-stroke position, the lateral confinement plates over which the rollers slide should be attached to the main beam so that the rollers coincide with the plates' axis. After measuring the distance from the transition elements' attachment point to the external border of the load cell in the horizontal position, the attachment point must be marked on the main beam in order to ensure that the attachment is made in the correct position, as close as possible to the actuator half-stroke position.

4.1.10. Installation of the Transition Elements on the Main Beam

Firstly, the complete retreat of the actuator (and consequently of the main test beam) must be carried out. This step aims to provide greater space for the installation of the transition elements and to guarantee that these elements will be installed in a position that does not interfere with the lateral confinement supporting elements, allowing for the use of the entire stroke of the actuator during the test. From the fixing markings made on the main beam, these elements must be installed with the help of the overhead crane. This fixation needs to be done in two stages, considering that the crane chains need to act in two positions: only on one side of the test beam (during the lifting of the load transfer assembly) and on both sides of the test beam (during system positioning for definitive fixation).

4.1.11. Counterweight Calibration

Firstly, the actuator stroke must be positioned close to the half-stroke, as this is the position where the counterweight must balance the load transfer subsystem. To better estimate the required counterweight load, the mass of the load transfer subsystem can be measured using a crane scale at the beam's suspension point. From this mass, the pulley system's conversion factor is applied (in this case, obtained analytically with a value near 57% of the load at the suspension point). With this estimation in mind, fine-tuning must be carried out by adding or subtracting small weights until it is possible to raise and lower the counterweight with approximately the same difficulty level (in this case, it was possible to perform this task manually without equipment).

4.1.12. Test Beam Leveling

After calibrating the counterweight, the beam's undisturbed position would not change unless some external force requested it. Therefore, the system should be leveled, and the vertical distance between the top of the concrete footing and the load cell axis should be measured. The confinement devices on the wall must be installed so that their axis is at the same elevation as the load axis. It should be noted that this dimension must coincide approximately with the axis of the reinforced concrete beam at the top of the wall, which must be considered when assembling the transition elements.

4.1.13. Fine-Tuning of Alignment with the Test Axis

Once the concrete footing has been positioned, the fine adjustment between the system's test axis and the wall's load axis can be made by adjusting the metallic elements' oblong holes in the direction orthogonal to the test plane. In the present case, two sets of oblong holes were made in the triangular load transition element: at the top (allowing adjustments of up to 2 cm in the connection between the triangle and the steel beam) and in the vertical part (allowing adjustments of up to 2 cm in the connection between the triangle and the hinge).

4.1.14. Confinement Devices Installation

After the horizontal and vertical adjustments, the actuator is slightly retracted, and the confinement devices are clamped to the wall, using rubber elements as intermediate layers. Four steel struts may be required to support these devices in the correct position after leveling in the two main directions.

4.1.15. Connection between the Transition Elements and the Confinement Device

Having defined the position of the confinement devices on the walls, check the level of the test beam and advance the actuator until the load cell plate touches the confinement device's plate. After some fine adjustments, the connection between the load transition elements and the wall confinement device is performed.

4.1.16. Installation of Overload Elements

The overload elements are then installed on top of the wall. Metal shims can be used to better support these elements on the concrete beam if there are irregularities on the surface. Next, the safety elements are connected to the overload elements and the test beam (or overhead crane) with steel cables with sufficient slack to allow the test movements without being stressed.

4.1.17. Assembly of the External Instrumentation Support Structure

The support structure is assembled to attend to the external instrumentation arrangement, that is, the positioning of the body of the sensors of types (i), (iii), and (iv). This structure must be attached to the reaction gantry through tensioned elements (wires, cables, or threaded rods).

4.1.18. Instrumentation Installation and Adjustments

After installing the sensors on the specimen, test system, and concrete footing, the sensors should be connected to the data acquisition system. After proceeding with the necessary settings in the data acquisition software, tests on the sensors are started, aiming to identify and replace defective sensors. In sequence, adjustments are made to the sensors, aiming to position the initial readings within the range of interest. In this case, type (i) and (iii) sensors were placed at mid-stroke, while type (ii) sensors were positioned, some at mid-stroke and others at 1/3 of the stroke, as some needed greater opening. Type (iv) sensors had a much higher available stroke than the expected displacements.

4.2. Testing the Specimen

This process can be broken down into the following activities: instrumentation verification, installation of cameras for recording, and conducting/monitoring the test.

4.2.1. Instrumentation Verification

Before starting the test, all of the sensors are checked, replacing them if necessary.

4.2.2. Installation of Cameras for Recording

The cameras for recording the test were positioned strategically, aiming to capture both the open and the more closed plans in three positions.

4.2.3. Conducting and Monitoring the Test

The test starts after programming the loading protocol and preparing the labels with the drifts on paper. The operators monitored throughout the entire test, continuously observing the evolution of damage to the specimen, registering the apparent damage and the corresponding drifts on the specimen with a marker pen. Periodically, notes and photographic records of the damage progression were taken. Safety aspects were also continuously observed, such as the stability of the damaged specimen, stiffness loss, and limit values of sensor displacements, among others. In the present experiments, the tests were conducted until significant evolution of the damage in the specimens was reached, going well beyond the deformations of the conventional limits of rupture in some cases (80% of the maximum force), without compromising safety. However, the criteria for ending the test are particular to each situation and must be defined before starting the test, with possible programming of stop protocols in the system software.

4.3. Demobilization

This process can be broken down into the following activities: disassembly, photographic record of damages, general verification of the test results/identification of improvement points, disconnecting the system from the confinement device, demolition and cleaning, removal of transition elements, and debris removal.

4.3.1. Disassembly

Once the test is concluded and the system is turned off, the sensors are removed, and their support elements (boxes and support structure) are dismantled. Overload elements are also demobilized from the top of the wall.

4.3.2. Photographic Record of Damages

Once free of the sensors and support elements, the specimen offers better viewing conditions and, thus, a detailed photographic record of the damage must be carried out.

4.3.3. General Verification of the Test Results and Identification of Improvement Points

The day after the test, a general verification and a primary analysis of the main test results are carried out (in this case, these results are forces and displacements at the top of the wall) to identify any anomalies and opportunities for improvement. In this way, learning is continuously incorporated into new test procedures.

4.3.4. Disconnecting the System from the Confinement Device

With the actuator turned on, the test system and the wall confinement device are disconnected, followed by the actuator retraction until the wall is isolated again. The specimen must be supported before disconnection from the test system if the wall conditions do not present sufficient stability. In the current study, the models were demolished in four points with reinforcements before the disconnection, and the overhead crane's chains were preventively attached to the steel bars.

4.3.5. Demolition and Cleaning

The next step is demolishing the tested wall, then cleaning the site. The demolition of reinforced masonry is facilitated as the reinforcement tends to maintain some integrity in the wall and allows it to be removed with the help of the overhead crane. Previously, however, cutting the rebars that connect the wall to the concrete base was necessary.

4.3.6. Removal of Transition Elements

Removing the transition elements is necessary to reconfigure the position of the components for a new test configuration, if applicable. In this way, if there are specimens to be tested, the preparation process for the test is restarted.

4.3.7. Debris Removal

The debris is removed if there are no new tests in the sequence.

5. Fundamental Analysis of Test System Outputs

The main outputs of the test system are force and displacement. As the system's degrees of freedom allow rotations that cause misalignment between the actuator's direction of action and the direction of wall movement, it was necessary to install a load cell next to the tested wall (orthogonal to it), in addition to installing external sensors for measuring displacements along the height of the wall, in the horizontal both main directions. In this way, it was possible to record the forces and displacements at the top of the specimens, making it possible to directly obtain cyclic diagrams of shear force x displacement on the walls.

Next, analyses on the behavior of forces, displacements, and force x displacement diagrams are presented, considering the illustrative cases of in-plane and out-of-plane shear tests, each performed separately on type C panels with plaster (specimens with labels CORP-C-CE-3 and CORFP-C-CE-3). As this is an exemplary case of the functioning of the system, the analyses were concentrated in the first half of the test, allowing for the contribution of the torsion effect on the wall to be neglected.

5.1. Actuator Forces × Load Cell Forces

It can be seen from the force × time graphs (Figure 20) that the forces registered along the wall have an evolution profile very similar to that of the actuator forces. However, they are slightly smaller, both in the pushing action (positive forces) and in the pulling action (negative forces), in both cases (in-plane—NP and out-of-plane—FP). It is important to remember that, due to the greater rigidity and, consequently, the more significant mobilization of forces relative to the displacements, from 15 min onwards, the in-plane tests were programmed to advance at a slower rate than the out-of-plane tests, which led to cycles of a longer duration in the NP configuration, from this moment on.

In the NP configuration, the first wall's plastification level seems to start around 30 min (25 mm displacements in the actuator). In contrast, the plastification level onset in the FP configuration points to 40 min (50 mm in the actuator). Because of the difference in inertia, damage evolution, and relative positioning of the reinforcements in the two horizontal directions of the cross-section of the panel, it is observed that the in-plane resisting forces were more significant than the out-of-plane forces, as expected.

Around 20 min into the test, the positive and negative forces presented some asymmetry, which increased with time in both cases. When on level ground, in the NP configuration, the forces in the pulling configuration were greater than the forces in the pushing configuration, whereas, in the FP configuration, the pushing forces exceeded the pulling forces.

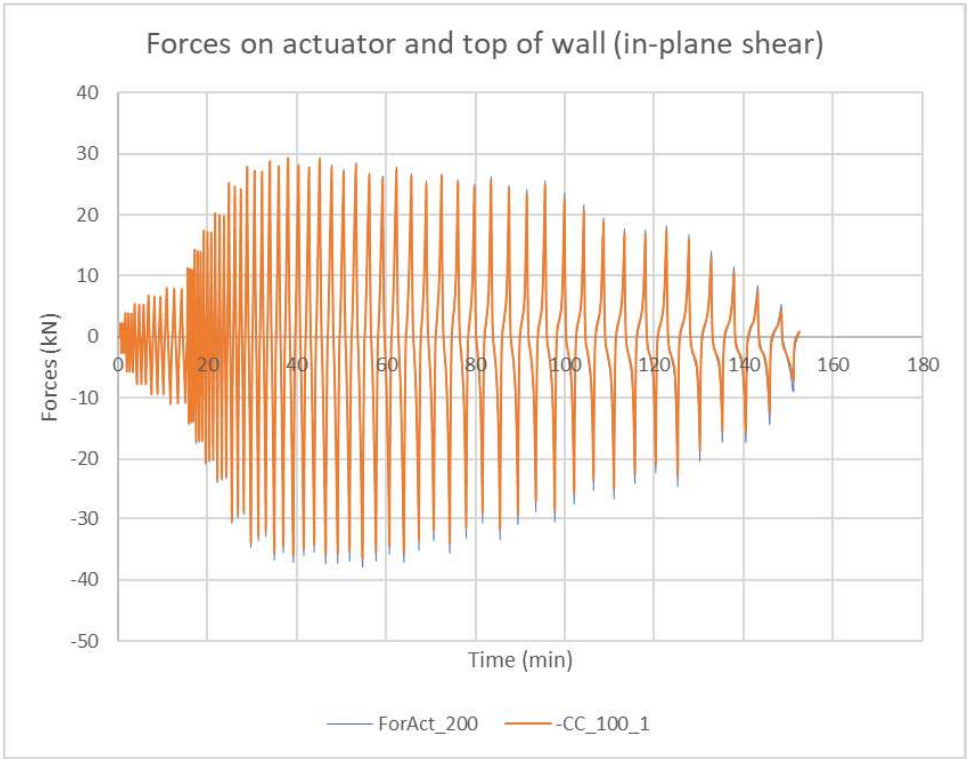

(**a**)

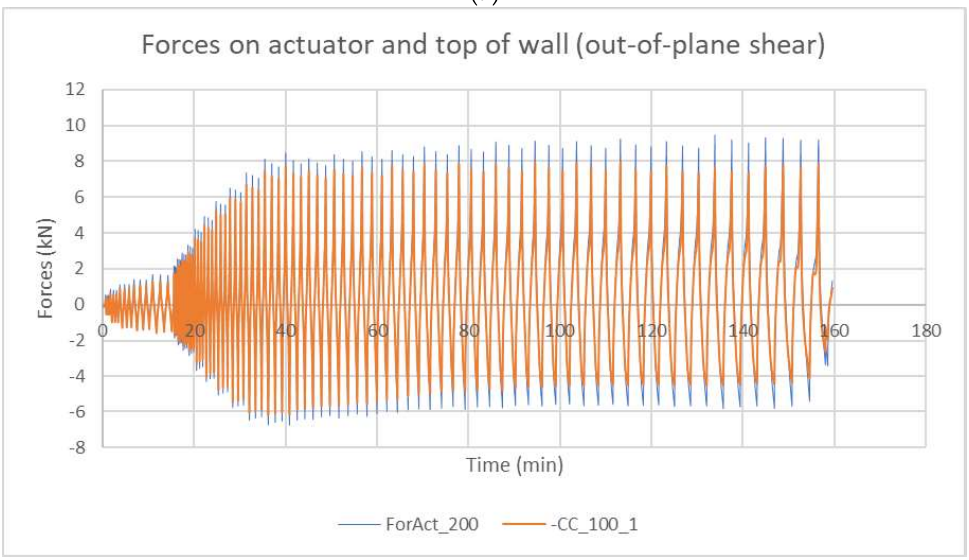

(**b**)

Figure 20. Comparison between the evolution of forces on the actuator and on the load cell near the top of the wall, in in-plane (**a**) and out-of-plane (**b**) configurations.

5.2. Displacements at the Actuator × Displacements at the Top of the Walls

The displacement × time graphs of the FP configuration (Figure 21b) showed similar values between the displacements of the actuator and the top of the wall (especially in the pulling configuration), with the displacements of the actuator being slightly higher. This behavior is similar to the NP behavior (Figure 21a) because the system rotations are higher in the pushing configuration, as the actuator acts in the same direction as the system rotation tendency, while in the pulling configuration, it operates in the opposite direction to the rotation tendency.

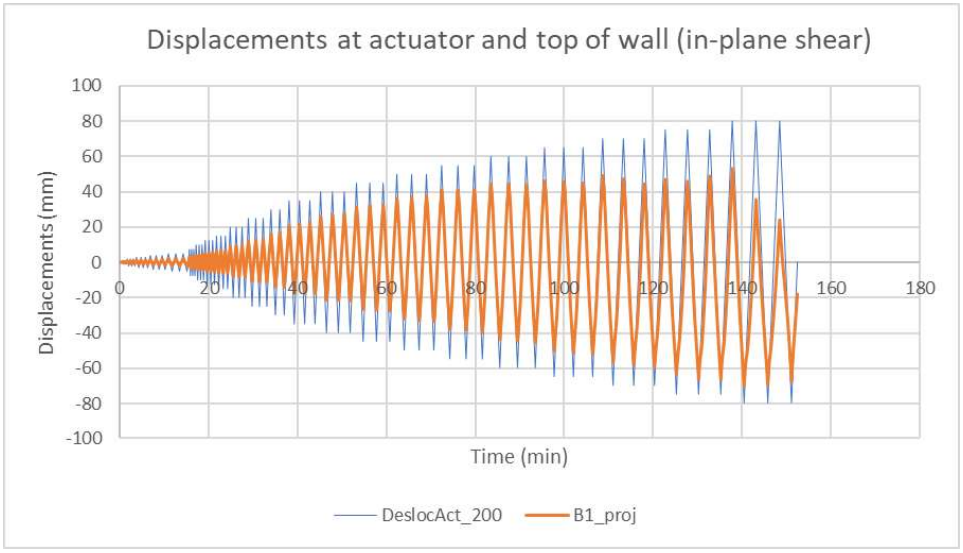

(**a**)

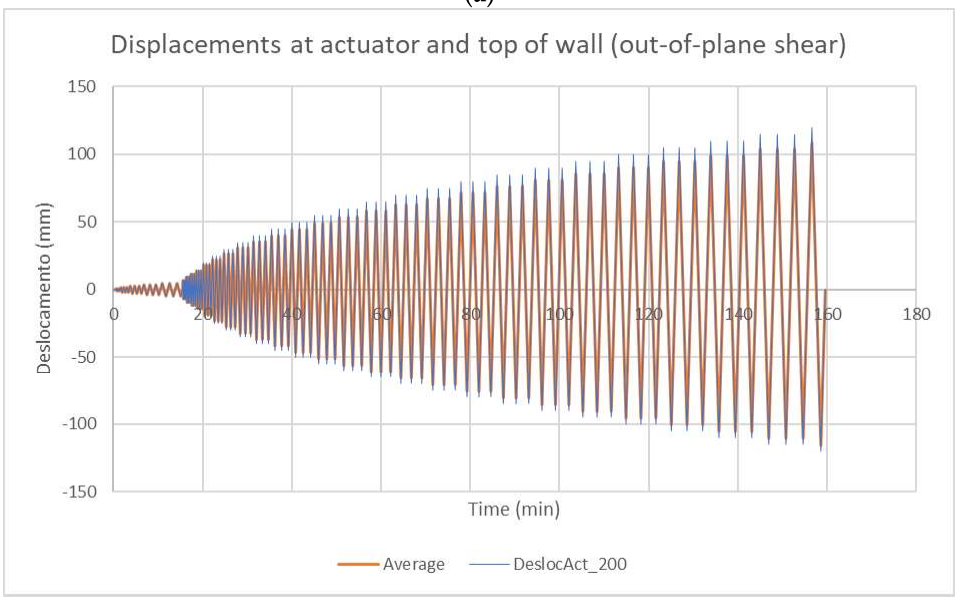

(**b**)

Figure 21. Comparison between the evolution of the displacements of the actuator and the top of the wall, in the in-plane (**a**) and out-of-plane (**b**) configurations.

In the NP configuration, the difference between these displacements was much higher in percentage, which reveals higher rotations in the test system. As the wall offers more shear resistance, its horizontal action on the triangular element rises, increasing the moment relative to the beam support in the gantry and, consequently, inducing rotations.

5.3. Force × Displacement Diagrams

From the diagrams in Figure 22, it can be seen that both in-plane and out-of-plane, the force × displacement diagrams of the actuator and the wall are similar and that the lag of forces is slight. It is also possible to state that the greater the rigidity, the greater the lag between the wall and actuator diagrams, mainly due to the difference in displacements caused by the system rotations, which are more significant for more rigid configurations.

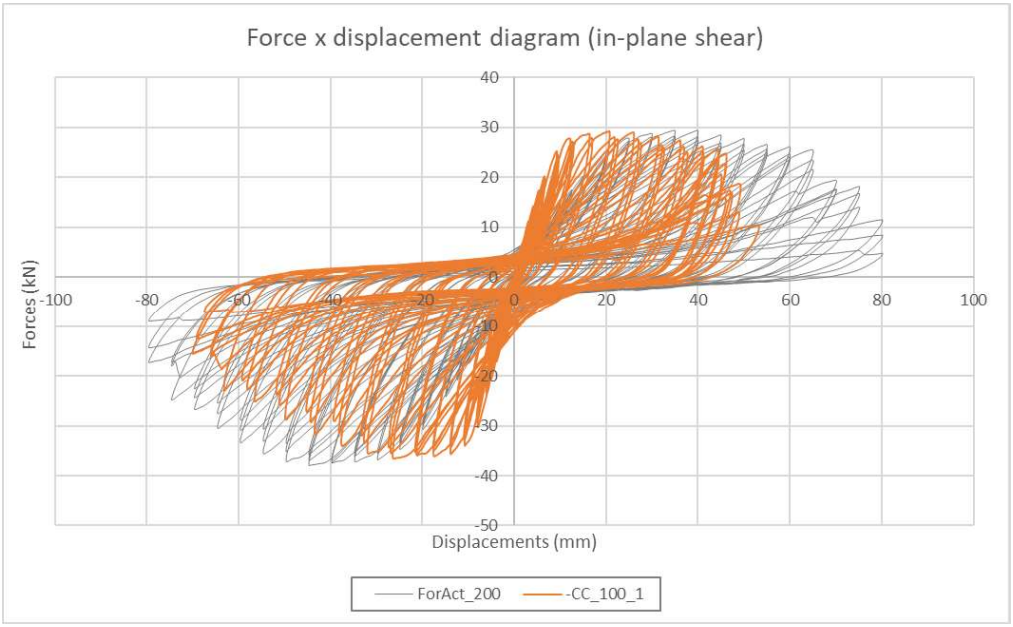

(**a**)

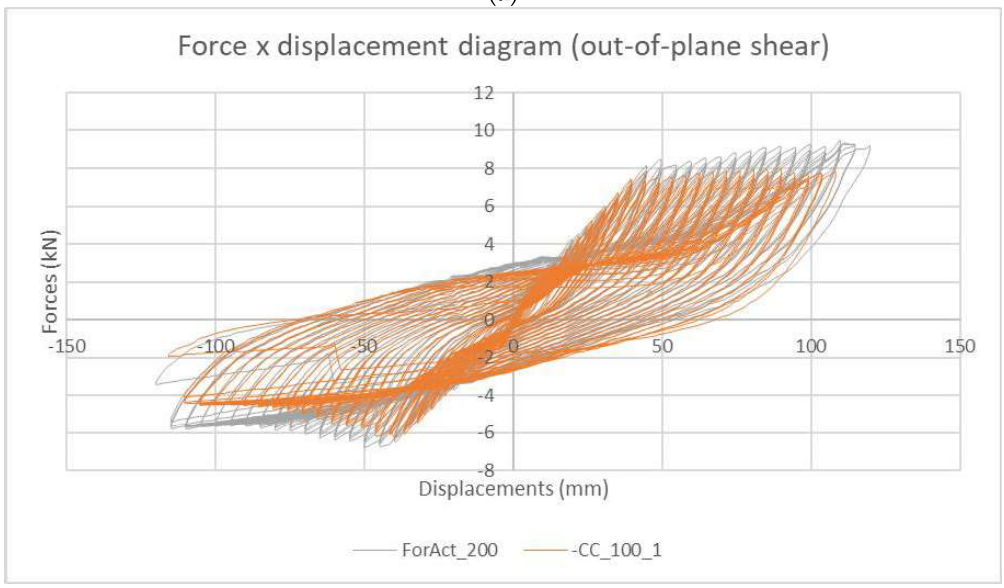

(**b**)

Figure 22. Comparison between force × displacement diagrams in in-plane (**a**) and out-of-plane (**b**) configurations.

6. Conclusions

The designed system made it possible to safely carry out cyclic shear tests on 15 walls in full scale, for an average of 8 days per specimen, bypassing substantial space restrictions and using local resources. In addition to the scalability aspect, the system needs only one servo-actuator (contrasting to other setups, which generally need three or four), providing a more viable setup where this resource limitation is a concern.

The proposed setup does not restrict rotations at the top, which is believed to better reflect the real operational conditions of the low-height buildings under seismic loads. Thus, the test reflects the shear behavior combined with bending and torsion (albeit partial) from applying the load on the axis that passes through the cross-section geometric center at the top of the wall. However, for the case of studying the wall's shear behavior in tall buildings, the proposed setup present design may not be the best choice as it does not provide the double-bending condition.

The main results of two representative specimens tested (in-plane and out-of-plane shear) were analyzed to illustrate the viability and peculiarities of the central test system's outputs.

It is helpful to remember that the function of the counterweight is precisely to facilitate the movement of the main test beam, reducing the vertical actions of the system on the wall. Even so, for the in-plane configuration, where the rotations of the system are more significant and the rotations on the wall are small, in the pushing configuration, the tendency is for the wall to restrict the rotations of the system and pull it down, reducing the compression and shear strength at the wall. Conversely, in the pulling configuration, the system tends to compress the wall, increasing the shear resistance.

In the out-of-plane configuration, where system rotations are smaller and wall rotations are more pronounced, in the pushing configuration, the system tends to restrict wall rotations and compress the wall, increasing shear resistance. Pulling results in the opposite, i.e., the normal force is reduced, and the shear resistance is lower.

The dynamics described above contribute, in part, to the asymmetries observed in both diagrams, which are also enhanced by the asymmetric evolution of damage on different sides of the specimen. It should be noted, however, that this type of asymmetry is a known fact in cyclic shear tests and that the results obtained are within the expected range.

However, it is understood that it is necessary to evaluate the system's performance for walls with a higher stiffness and obtain the system performance limits in terms of force and displacement. The future research plan also includes modeling and the study of uncertainties, as well as improving the setup design.

Supplementary Materials: The following supporting information can be downloaded at: https://www.mdpi.com/article/10.3390/app13137498/s1, Video S1: SHS Test System (2022).

Author Contributions: Conceptualization, L.D.G., A.C., H.R. and J.F.; methodology, L.D.G., A.C., H.R., J.F. and A.T.C.; formal analysis, L.D.G., A.C. and H.R.; investigation, L.D.G., A.C., H.R., J.F. and A.T.C.; resources, L.D.G., A.C., H.R. and A.T.C.; writing—original draft preparation, L.D.G.; writing—review and editing, L.D.G., A.C., H.R., J.F. and A.T.C.; supervision, L.D.G., A.C. and H.R.; project administration, L.D.G. and A.C.; funding acquisition, L.D.G., A.C., H.R. and A.T.C. All authors have read and agreed to the published version of the manuscript.

Funding: Leandro Di Gregorio thanks the SHS Project's team and the Federal University of Rio de Janeiro/Polytechnic School for his postdoctoral work license. The authors acknowledge the funding of the Civil Construction Department of POLI UFRJ used in manufacturing the blocks and constructing the specimens. The authors also acknowledge UA Civil Engineering Department for the use of Lab facilities and Vagoinertes, LDA., which provided the soil, water, electricity, and storage. This work was also supported by the Foundation for Science and Technology (FCT)—Aveiro Research Centre for Risks and Sustainability in Construction (RISCO), Universidade de Aveiro, Portugal [FCT/UIDB/ECI/04450/2020]. Alice Tavares developed her part of the work within the scope of the project CICECO, Aveiro Institute of Materials, UIDB/50011/2020, UIDP/50011/2020, and LA/P/0006/2020 and 2021.03830. CEECIND is financed by national funds through the FCT/MCTES (PIDDAC). Moreover, Jorge Fonseca acknowledges the Foundation for Science and Technology (FCT) for the PhD grant, with reference 2022.13794.BD.

Institutional Review Board Statement: Not applicable.

Data Availability Statement: The data presented in this study are available upon request from the corresponding author.

Conflicts of Interest: The authors declare no conflict of interest.

References

1. Oliveira, C.S.; Ferreira, M.A.; Sá, F.M. Earthquake Risk Reduction: From Scenario Simulators Including Systemic Interdependency to Impact Indicators. In *Perspectives on European Earthquake Engineering and Seismology*; School of Engineering Ozyeğin, University Istanbul: Istambul, Turkey, 2014.
2. IPCC. Summary for Policymakers. In *Global Warming of 1.5 °C. An IPCC Special Report on the Impacts of Global Warming of 1.5 °C above Pre-Industrial Levels and Related Global Greenhouse Gas Emission Pathways, in the Context of Strengthening the Global Response to the Threat of Climate Change*; Cambridge University Press: Cambridge, UK; New York, NY, USA, 2018; pp. 3–24.

3. Heintze, H.J.; Kirch, L.; Küppers, B.; Mann, H.; Mischo, F.; Mucke, P.; Pazdzierny, T.; Prütz, R.; Radtke, K.; Strube, F.; et al. *World Risk Report 2018*; Bündnis Entwicklung Hilft: Berlin, Germany; Ruhr University: Bochum, Germany, 2018.
4. Le Maoult, A.; Politopoulos, I.; Atanasiu, G.M.; Casarotti, C.; Pavese, A.; Dorka, U.; Nguyen, V.T.; Marazzi, F.; Molina Ruiz, F.; Pegon, P. *EFAST Project (Design Study of a European Facility for Advanced Seismic Testing)*; 1st Year EFAST Annual Report; European Union: Brussels, Belgium, 2010.
5. Gregorio, L.T.; Guimarães, G.V.D.M.; Danziger, F.A.B.; Jannuzzi, G.M.F.; Qualharini, E.L.; Veról, A.P.; Haddad, A.N.; Miguez, M.G.; Cruz, V.N.; Bianchessi, D.I. Simple Housing Solution Project: (Re) Building in Critical Situations. In *Natural Hazards*; Intechopen: London, UK, 2020. [CrossRef]
6. United Nations Office for Disaster Risk Reduction. Sendai Framework for Disaster Risk Reduction 2015–2030. Available online: https://www.undrr.org/publication/sendai-framework-disaster-risk-reduction-2015-2030 (accessed on 27 May 2023).
7. Tenório, M.C.U. *Análise da Viabilidade Técnica da Alvenaria Estrutural em Tijolos de Solo-Cimento para Situações com Cargas Sísmicas: Práticas Construtivas e Análise Estrutural do Projeto de Solução Habitacional Simples*; Undergraduate Monograph in Civil Engineering; Federal University of Rio de Janeiro: Rio de Janeiro, Brazil, 2019.
8. UNH—United Nations. Habitat II, the Second United Nations Conference on Human Settlements. June 3 to 14, 1996 in Istanbul, Turkey. Available online: http://habitat.scarp.ubc.ca/habitat-ii-conference/ (accessed on 29 May 2023).
9. UNISDR. Risk and Poverty in a Changing Climate. Global Assessment Report on Disaster Risk Reduction. 2009. Available online: http://www.preventionweb.net/english/hyogo/gar/report/index.php?id=9413 (accessed on 29 May 2023).
10. UNESCO. Managing Disaster Risks for World Heritage. 2010. Available online: https://whc.unesco.org/en/managing-disaster-risks/ (accessed on 29 May 2023).
11. Di Gregorio, L.T.; Guimarães, G.V.D.M.; Tenório, M.C.U.; Lima, D.; Haddad, A.N.; Danziger, F.A.B.; Jannuzzi, G.M.F.; Santos, S.H.; Lima, S.S. The Potential of CEB Reinforced Masonry Technology for (Re)construction in the Context of Disasters. *Materials* **2020**, *13*, 3861. [CrossRef]
12. Vintzileou, E. Testing Historic Masonry Elements and/or Building Models. In *Perspectives on European Earthquake Engineering and Seismology*; School of Engineering Ozyeğin, University Istanbul: Istanbul, Turkey, 2014.
13. NIKER Project. Available online: https://cordis.europa.eu/project/id/244123/reporting (accessed on 17 April 2023).
14. Van Vliet, M.R.A. *Shear Tests on Masonry Panels*; Literature Survey and Proposal for Experiments; TNO Report 2004-CI-R0171; TNO: The Hague, The Netherlands, 2004.
15. Gallegos, H.; Casabonne, C. Cyclic test on three different types of masonry walls. In Proceedings of the 4th Canadian Masonry Symposium, Fredericton, NB, Canada, 2–4 June 1986.
16. Richardson, J.; Dave, J.L. Experimental investigation of the behaviour of masonry infilled steel framessubjected to cyclic racking loads. In Proceedings of the 4th Canadian Masonry Symposium, Fredericton, NB, Canada, 2–4 June 1986.
17. Kaminosono, T.; Isoishi, H.; Yamaguchi, Y.; Kawai, R. Seismic capacity of reinforced masonry walls including effects of axial stress. In Proceedings of the 4th Canadian Masonry Sumposium, Fredericton, NB, Canada, 2–4 June 1986.
18. Fujisawa, M.; Kawashima, T.; Yamaguchi, Y. Seismic capacityod reinforced masonry walls; effect of shear span ratio. In Proceedings of the 4th Canadian Masonry Symposium, Fredericton, NB, Canada, 2–4 June 1986.
19. Magenes, G.; Calvi, G.M. Cyclic behaviour of brick masonry walls. In Proceedings of the 10th World Conference on Earthquake Engineering, Madrid, Spain, 19–24 July 1992; pp. 3517–3522.
20. Bosiljkov, V.; Page, A.; Bosiljkov, V.B.; Zarnic, R. Performance based studies of in-plane loaded Unreinforced masonry walls. *J. Mason. Int.* **2003**, *16*, 39–50.
21. Loring, A.O.E.S. *Tastversuche zur Identifizierung des Verhaitensfaktors von Mauerwerksbauten fur den Erdbebennachweis*; University of Dortmund: Dortmund, Germany, 2003.
22. Modena, C.; Da Porto, E.F.; Garbin, F. *Test Report*; University of Padua: Padua, Italy, 2004.
23. Modena, C.; Da Porto, E.F.; Garbin, F. *Ricerca Sperimentale sul Comportamento di Sistemi per Muratura Portante in Zona Sismica*; University of Padua: Padua, Italy, 2005.
24. Magenes, G.; Morandi, P.; Penna, A. *Test Results on the Behaviour of Masonry under Static Cyclic in Plane Lateral Loads*; University of Pavia: Pavia, Italy, 2008.
25. Frumento, S.; Magenes, G.; Morandi, P.; Calvi, G.M. *Interpretation of Experimental Shear Tests on Clay Brick Masonry Walls and Evaluation of q-Factors for Seismic Design*; Istituto Universitario di Studi Superiori di Pavia: Pavia, Italy, 2009.
26. Seki, M.; Vacareanu, R.; Saito, T.; Cotofana, D.; Lozinca, E.; Popa, V.; Chesca, A.B. Cyclic Shear Tests on Plainand FRP Retrofitted Masonry Walls. In Proceedings of the 14th World Conference on Earthquake Engineering, Beijing, China, 12–17 October 2008.
27. Magenes, G.; Penna, A.; Galasco, A.; Da Paré, M. In-plane cyclic shear tests of undressed double-leaf stone masonry panels. In Proceedings of the 8th International Masonry Conference, Dresden, Germany, 4 July 2010.
28. Maida, Y.; Sakata, H.; Qu, Z.; Maegawa, T.; Suzuki, H. Cyclic loading test of lightly reinforced concrete wall piers with slit dampers in RC frames. *Eng. Struct.* **2021**, *236*, 112099. [CrossRef]
29. Ferretti, F.; Jafari, S.; Esposito, R.; Rots, J.G.; Mazzotti, C. Critical analysis on the use of the shove test for investigating the shear-sliding behavior of brick masonry. *Eng. Struct.* **2022**, *254*, 113860. [CrossRef]
30. Lanese, I.; Pavese, A.; Furinghetti, M. Hybrid testing of Seismic Isolated Structures: Facing time and Geometry Scaling Issues. In Proceedings of the 1st European Conference on Earthquake Engineering, Thessaloniki, Greece, 19–21 June 2018.

31. Mucciarelli, M. The Role of Site Effects at the Boundary Between Seismology and Engineering: Lessons from Recent Earthquakes. In *Perspectives on European Earthquake Engineering and Seismology*; School of Engineering Ozyeğin, University Istanbul: Istambul, Turkey, 2014.
32. Scrum Alliance. What Is SCRUM? An Agile Framework for Completing Complex Projects. Available online: https://www.scrumalliance.org/about-scrum (accessed on 20 April 2023).
33. Di Gregorio, L.T.; Costa, A.G.; Tavares, A.; Rodrigues, H.; Fonseca, J. SHS-Multirisk UFRJ-UA: Simple Housing Solution for (re)construction resilient to earthquakes and hurricanes. In Proceedings of the 9° Fórum Internacional do Patrimônio Arquitetônico, Portugal, Brazil, 14–16 June 2023.
34. Yang, C.; Liang, K.; Zhang, X.; Geng, X. Sensor placement algorithm for structural health monitoring with redundancy elimination model based on sub-clustering strategy. *Mech. Syst. Signal Process.* **2019**, *124*, 369–387. [CrossRef]
35. Yang, C.; Ouyang, H. A novel load-dependent sensor placement method for model updating based on time-dependent reliability optimization considering multi-source uncertainties. *Mech. Syst. Signal Process.* **2022**, *165*, 108386. [CrossRef]
36. Yang, C.; Xia, Y. Interval Uncertainty-Oriented Optimal Control Method for Spacecraft Attitude Control. *IEEE Trans. Aerosp. Electron. Syst.* **2023**, 1–13. [CrossRef]
37. Yang, C.; Lu, W.; Xia, Y. Reliability-constrained optimal attitude-vibration control for rigid-flexible coupling satellite using interval dimension-wise analysis. *Reliab. Eng. Syst. Saf.* **2023**, *237*, 109382. [CrossRef]